EVCSEL URO Day-2013

May 31st-June 1st 2013

Lausanne, Switzerland

In cooperation with the CTI

Beam eXpress

U·L·M PHOTONICS

SWISS PHOTONICS

KTT-Support
National thematic networks

Schweizerische Eidgenossenschaft
Confédération suisse
Confederazione Svizzera
Confederaziun svizra

Swiss Confederation

Commission for Technology and Innovation CTI

Program

Friday			
8:30	Welcome @ room MXF1		
8:50	Eli Kapon	EPFL	Welcome presentation
	Nitrides, micro waves		Chair: Raphaël Butté
9:00	Åsa Haglund	Chalmers University of Technology	*Transverse Optical Guiding in GaN-based Vertical-Cavity Surface-Emitting Lasers*
9:20	Angel Valle	Univ. de Cantabria	*Dynamics of VCSELs subject to dual-beam optical injection*
9:40	Xi Zeng	CSEM	*Injection-seeded long external cavity InGaN/GaN surface-emitting laser at 420 nm wavelength*
10:00	Gatien Cosendey	EPFL	*Monolithic InAlN-based blue VCSELs*
10:20	Coffee break		
	Industry		Chair: Tony Weidberg
10:40	Angélique Rissons	ISAE	*VCSEL for space systems*
11:00	Vincent Lecocq	Innoptics SAS	*Hermetic packaging of a twelve-channel high bit rate VCSEL based transceiver*
11:20	Markus Ortsiefer	Vertilas	*Recent Progress of InP-based Long-Wavelength VCSELs for Communications Applications*
11:40	Vladimir Iakovlev	EPFL	*Progress and challenges in industrial fabrication of wafer-fused VCSELs*
12:00	Ulrich Weichmann	Philips Technologie GmbH	*High power VCSEL Systems*
12:20	Rainer Strzoda	Siemens AG	*Miniature low-cost platform for volume applications in VCSEL-based gas sensing*
12:40	Christophe Bonneville	Resolution Spectra Systems	*SWIFTS technology: A new tool for VCSEL spectrum analysis*
13:00	Lunch @ *Ornithorynque*		
	Telecom/Datacom		Chair: Åsa Haglund
14:00	Kent Choquette	University of Illinois at Urbana-Champaign	*Challenges and Progress toward 50Gb/s-km VCSEL Modulation*
14:20	Erik Haglund	Chalmers University of Technology	*High-speed 850 nm datacom VCSELs*
14:40	Silvia Spiga	Technische Universität München	*Epitaxial-Stacked Double-Active Region in InP-based 1.55 μm Short-Cavity VCSELs for High-Speed Data Transmission*
15:00	Dalila Ellafi	EPFL	*Impact of Cavity Photon Lifetime on High Speed performance of 1.3-μm Wavelength Wafer-Fused VCSELs*
15:20	Philip Moser	Technische Universität Berlin	*Energy efficient 850 nm VCSELs for Data and Computer Communication*
15:40	J.A. Lott	Technische Universität Berlin	*Infrared VCSELs for Short Distance High Bit Rate Free Space Optical Interconnects*
16:00	Coffee break		
	Simulations		Chair: Angélique Rissons
16:20	Nicolas Volet	EPFL	*Improved single-mode emission characteristics of long-wavelength wafer fused VCSELs by intra-cavity patterning*
16:40	Werner Hofmann	Technische Universität Berlin	*Scalability challenges of VCSEL-based optical interconnects*
17:00	Jaroslaw Walczak	Lodz University of Technology	*On-axis pumped VECSEL with double diamond heatspreader*
17:20	Tony Weidberg	CERN	*VCSEL reliability and understanding VCSEL failure mechanisms under humidity*
17:40	Tomasz Czyszanowski	Lodz University of Technology	*Antiguided VCSEL arrays*
19:00	Dinner @ *Ornithorynque*		
21:00	Bedtime		

Saturday			
	High contrast gratings		Chair: Kent Choquette
9:00	Il-Sug Chung	Technical University of Denmark	*Hybrid VCSEL using grating mirrors*
9:20	Marcin Gebski	Lodz University of Technology	*GaAs/AlOx and Si/SiOx high contrast gratings for 980 nm VCSELs*
9:40	Pierluigi Debernardi	Politecnico di Torino	*Performance of 980 nm VCSELs with different High-Contrast-Gratings*
10:00	Coffee break		
10:20	Christophe Levallois	Université Européenne de Bretagne	*VCSEL based on InAs Quantum-Dashes with an Emission Spectral Width of 105-nm*
10:40	Corrado Sciancalepore	CNRS - Université de Lyon	*High-contrast metastructures for VCSEL photonics on silicon*
11:00	Yi Xie	Ghent University	*VCSEL with switchable transverse and longitudinal modes*
11:20			*VCSEL day wrap up and conclusion*
12:00			*Lunch (Picnic @ Esplanade)*

Technical Committee

M. Adams, M.-C. Amann, D. Bimberg, I.-S. Chung, N. Grandjean, E. Kapon, A. Larsson, J. Lott, R. Michalzik, A. Rissons and P. Viktorovitch

Organization Committee

P. Gallo, E. Kapon, A. Rudra, A. Sirbu and N. Volet

Location

Nitrides and Microwave generation

Session chair : Raphaël Butté

Engineering the Transverse Optical Guiding in GaN-Based Vertical-Cavity Surface-Emitting Lasers to Reach the Lowest Threshold Gain

Ehsan Hashemi[1], Johan Gustavsson[1], Jörgen Bengtsson[1], Martin Stattin[1], Gatien Cosendey[2], Nicolas Grandjean[2], and Åsa Haglund[1]

[1] *Photonics Laboratory, Department of Microtechnology and Nanoscience, Chalmers University of Technology, Sweden*
[2] *Laboratory of Advanced Semiconductors for Photonics and Electronics, École Polytechnique Fédérale de Lausanne, Switzerland*

Keywords: Optical guiding, GaN laser, blue microcavity, vcsel.

GaN-based vertical-cavity surface-emitting lasers (VCSELs) emitting in the blue-green regime have been difficult to realize, and few groups have so far demonstrated electrically injected blue VCSELs lasing at room temperature[1-5], with fairly high threshold current densities and low output powers. In these lasers, transverse current confinement is achieved by having an opening in a current blocking layer – a current aperture – placed between the p-doped intracavity contact layer and indium-tin-oxide layer. There are reasons to believe that this type of current aperture lowers the degree of transverse optical guiding, and even results in anti-guided structures with high leakage losses and thereby is a strong contributing factor to the high threshold current densities typically seen in these devices.

In this work, three different current aperture schemes were studied: (a) dielectric Si_xN_y or SiO_2 aperture[1-5]; (b) epitaxial AlN[7] or $AlInN$[8] aperture using regrowth; (c) oxide aperture by selective oxidation of $AlInN$[9], with a GaN-based VCSEL structure similar to the one proposed by EPFL[6] as a starting point. For these cavities, the transverse effective index difference, Δn_{eff}, and threshold material gain are calculated using a quasi-two-dimensional (2D) effective index method and a three-dimensional (3D) coupled-cavity beam propagation method. The aperture scheme (a), the most commonly used design, and scheme (b) introduce a depression of the structure near the optical axis, which yields optically anti-guided structures, i.e. with $\Delta n_{eff} <0$, while scheme (c) provides a planar structure (assuming no expansion or contraction of the oxidized layer) and therefore results in positive guiding, since $n_{oxide} < n_{p\text{-}GaN}$. Remarkably, increased degree of anti-guiding dramatically reduces the threshold material gain, which can be attributed to mainly a reduction of transverse leakage of optical power. However, in such anti-guided devices the threshold material gain is very sensitive to small changes in optical guiding introduced by thermal lensing effects, small deviations in fabrication etc. To realize more robust devices and reduce the threshold material gain further by entirely avoiding the transverse leakage, new designs are proposed that involve planarization of the structure or introducing an elevation near the optical axis. These structures can yield the desired moderate positive guiding with $\Delta n_{eff} \sim 0.015\text{-}0.020$, which is at a safe distance from the antiguiding catastrophe near $\Delta n_{eff} =0$ and will reduce the material threshold gain from 4000-6000 cm^{-1}, for antiguided cavities, down to 2000 cm^{-1}, which will be important in the realization of GaN-based VCSELs with low threshold current densities.

References

1. D. Kasahara et al., *Appl. Phys. Express* **4**, 072103 (2011).
2. S. C. Wang et al., *Proc. SPIE* **8276**, 827607 (2012).
3. T. Onishi et al., *IEEE J. Quantum Electron.* **48**, 1107 (2012).
4. C. Holder et al., *Appl. Phys. Express* **5**, 092104 (2012).
5. G. Cosendey et al., *Appl. Phys. Lett.* **101**, 151113 (2012).
6. R. Butté et al., *Proc. SPIE* **7216**, 721619 (2009).
7. B. S. Cheng et al., *Appl. Phys. Lett.* **99**, 041101 (2011).
8. W. S. Tan et al., *Appl. Phys. Express* **2**, 112101 (2009).
9. A. Castiglia et al., *Appl. Phys. Lett.* **90** 033514 (2007)

Dynamics of VCSELs subject to dual-beam optical injection

A. Quirce[1], A. Consoli[2], P. Pérez[1], I. Noriega[1], **A. Valle**[1], L. Pesquera[1] and I. Esquivias[2]

[1] *Instituto de Física de Cantabria, CSIC-Univ. Cantabria, Avda. Los Castros s/n, E-39005, Santander, Spain.*
[2] *Departamento de Tecnología Fotónica, Universidad Politécnica de Madrid, ETSI de Telecomunicación, Ciudad Universitaria, 28040, Madrid, Spain.*

Keywords: VCSEL*, optical injection, nonlinear dynamics.*

Vertical-cavity surface-emitting lasers subject to single optical injection exhibits various nonlinear dynamics including stable locking, periodic and chaotic oscillations[1]. Period-one nonlinear dynamics of optically injected semi conductor lasers has been used for microwave signal generation[2]. This approach allows widely tunable, optically controlled and single sideband generation of microwave signals. Dual-beam optical injection in semiconductor lasers has recently attracted much attention due to the use of DFB lasers to generate microwave signals with frequencies corresponding to the frequency differences between the two master lasers (MLs)[3].

In this work we report an experimental and theoretical study of the nonlinear dynamics of a 1550 nm single-transverse mode VCSEL subject to two-frequency optical injection. The directions of the polarizations of ML1 and ML2 are orthogonal to the direction of the polarization of the VCSEL lasing mode. In Fig. 1 we show that the VCSEL can emit in the two MLs wavelengths in such a way that the frequency of the generated microwave signal corresponds to the frequency difference between the two MLs. Peaks in the optical spectrum of the injected VCSEL are clearly larger than the peaks that correspond to the reflected light of ML1 and ML2 at the VCSEL's mirror. Polarization switching (PS) of the VCSEL to the polarization direction of the two MLs is observed. Period-one and period-two dynamics with PS are found when the ML2 wavelength, λ_{ML2}, is tuned over wide ranges while λ_{ML1} is fixed to a value for which there is locking with PS under single optical injection. If λ_{ML1} is changed such that there is not such a locking, tuning of λ_{ML2} leads to much more complex dynamics in both polarizations. Very good agreement is found between our experimental and theoretical results.
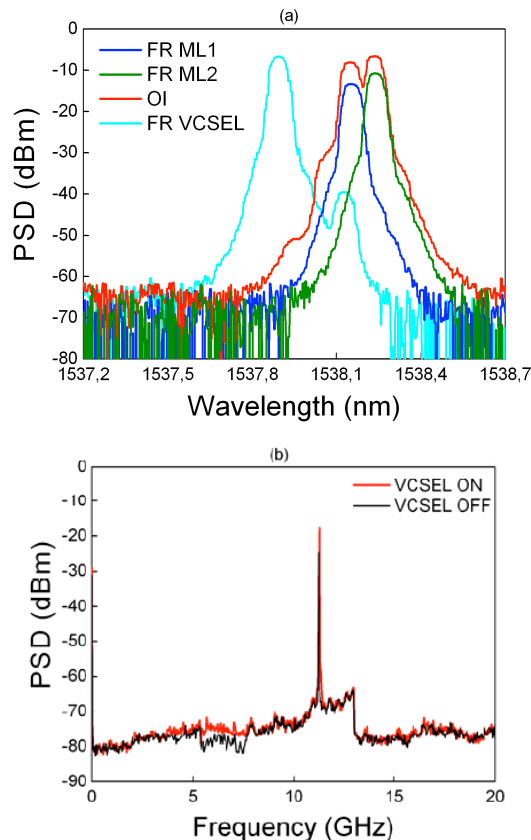

Figure 1. Optical spectrum (a) of the free running ML1 (blue line), ML2 (green line) and VCSEL (cyan line) and of the two frequency injected VCSEL (red line), with I_{VCSEL} = 4.0 mA, λ_{ML1}= 1538.15 nm and λ_{ML2} = 1538.24 nm. Electrical spectrum (b) obtained from the two frequency injected VCSEL (red) and from the same set-up but with the VCSEL off (black).

References
1. J. Buesa, I. Gatare, K. Panajotov, H. Thienpont, M. Sciamanna, *IEEE J. Quantum Electron*., **42**, 198 (2006)
2. X. Q. Qi and J. M. Liu, *IEEE J. Sel. Topics Quantum Electron.*, **17**, 1198 (2011)
3. Y. S. Juan, F. Y. Lin, *IEEE Photonics J*. **3**, 644 (2011)

Injection-seeded long external cavity InGaN/GaN surface-emitting laser at 420 nm wavelength

X. Zeng[1,2], D. L. Boïko[1], G. Cosendey[2], M. Glauser[2], J.-F. Carlin[2] and N. Grandjean[2]

[1]Centre Suisse d'Électronique et de Microtechnique SA (CSEM), Jaquet-Droz 1, CH-2002 Neuchâtel, Switzerland, email : xi.zeng@csem.ch, dmitri.boiko@csem.ch
[2]Institute of Condensed Matter Physics (ICMP), École Polytechnique Fédérale de Lausanne (EPFL), CH-1015 Lausanne, Switzerland

Keywords: VECSEL, external cavity laser, III-nitride, injection seeding

Vertical-external-cavity surface-emitting lasers (VECSELs) incorporate many attractive features of both semiconductor and solid state lasers such as the ability to achieve high output power simultaneously with high quality circular-shaped output beam.[1] To cover the blue to UV spectrum, VECSELs based on group III-nitrides are needed. Existing literature on nitride-based VECSELs report cavity lengths on the order of 2 mm or less.[2,3] Placing intracavity elements (e.g. saturable absorber for modelocking) in these VECSELs would be very difficult due to their extremely short cavity lengths.

The difficulty of achieving lasing in a nitride-based VECSEL with longer cavity lengths lies in the general unavailability of high power (>1 W) continuous wave lasers at UV wavelengths that are used as the optical pump source. Pulsed UV lasers are typically used. However, for a III-nitride VECSEL, the time required for lasing modes to build up in a 50 mm long cavity is ~680 ns when pumped at twice the threshold according to calculations found in Reference 4. At the same time, high power pulsed UV lasers typically have pulse durations of 10 ns or less. Thus, obtaining lasing from a standalone 50 mm long VECSEL would not be possible because the pump pulses do not last long enough. In contrast, the build up time of lasing emission in a monolithic VCSEL cavity is much shorter at 10 ps or less. Therefore, we overcome the difficulties of achieving lasing in long cavity VECSELs by forming an auxiliary microcavity to provide injection seeding for the external cavity mode at early stages of the lasing build up. This is done by depositing a partially transmitting top DBR.

Here, we report optically pumped InGaN/GaN quantum well (QW) VECSELs with latticed-matched AlInN/GaN bottom distributed Bragg reflector (DBR), dielectric-based partially transmitting top DBR (at 7 and 4 periods), and external mirror (curvature ρ=50 mm, reflectivity R=99.5% at 420 nm) at cavity lengths of up to 50 mm (semiconfocal cavity configuration). Lasing is achieved at 420 nm wavelength under pumping by 400 ps or 10 ns pulses at 355 nm. The spectra and quality factor of the VECSEL output beam give evidence of external cavity mode lasing.

Under pumping by 400 ps duration pulses, we find the VECSEL lasing threshold (peak) powers to be on the order of ~20 W and ~90 W for the 7 and 4 period top DBR samples, respectively. Optical pumping by 10 ns duration pulses significantly reduces the lasing thresholds to 1.26 W and 2.57 W for the 7 and 4 period top DBR samples, respectively. The reduction in threshold pump power by a factor of ~17 is clearly seen in Fig. 1, where the normalized L-L curves of the 7-period top DBR sample in semiconfocal VECSEL configuration are plotted. Detailed explanation of threshold reduction mechanism for different pump pulse lengths is given in Reference 5.

Beam quality measurements are made for the same two VECSELs at cavity length of 49 mm, 35 mm and 25 mm. Figure 2 shows the extracted M^2 values. The M^2 value is significantly smaller than that of a VCSEL without external cavity mirror (shown in Fig. 2 at zero cavity length). The cavity length 49 mm gives the lowest $M^2 \sim 1.0$ for the 7-period top DBR sample. This is the expected result for a cavity approaching the semiconfocal configuration.
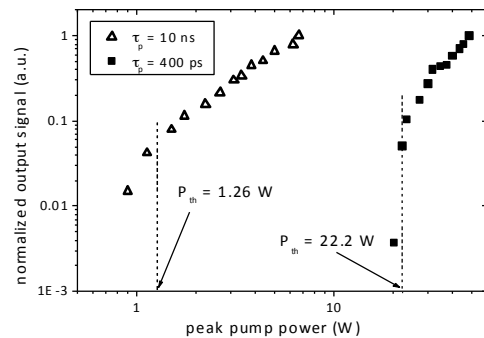

Fig. 1 – L-L measurement data for 7-top DBR sample in semiconfocal VECSEL configuration, pumped by frequency-tripled Nd:YAG lasers with pulse lengths 10 ns (triangles) and 400 ps (squares). Peak threshold powers are 1.26 W and 22.2 W, respectively.
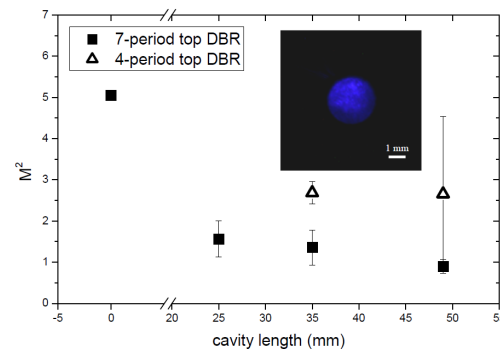

Fig. 2 – Extracted M^2 values plotted as a function of cavity length. Inset: The beam emitted from a 49 mm cavity length VECSEL with 7-period top DBR, measured at distance of 123 mm from the sample.

In conclusion, we report operation of a group III-nitride vertical-external-cavity surface-emitting laser with supporting evidence of external cavity operation. Achievable external cavity length of up to 50 mm is large enough for placement of intracavity elements, e.g. a saturable absorber, making our device a suitable testbed in various experiments involving the wavelength range reachable by III-nitride semiconductors.

References

[1]A. Laurain, M. Myara, G. Beaudoin, I. Sagnes, and A. Garnache, Optics Express **18** (14), 14627 (2010).
[2]R. Debusmann, N. Dhidah, V. Hoffmann, L. Weixelbaum, U. Brauch, T. Graf, M. Weyers, and M. Kneissl, IEEE Photonics Technology Letters **22** (9), 652 (2010).
[3]T. Wunderer, J. E. Northrup, Z. Yang, M. Teepe, A. Strittmatter, N. M. Johnson, P. Rotella, and M. Wraback, Applied Physics Letters **99** (20), 201109 (2011).
[4]A. E. Siegman, *Lasers* (University Science Books, Sausalito, CA, 1986).
[5]X. Zeng, D. L. Boïko, G. Cosendey, M. Glauser, J.-F. Carlin, and N. Grandjean, Journal of Applied Physics **113** (4), 043108 (2013).

Monolithic InAlN-based blue VCSELs

G. Cosendey, A. Castiglia, M. Glauser, J.-F. Carlin, R. Butté, and N. Grandjean

Laboratory of Advanced Semiconductors for Photonics and Electronics, École Polytechnique Fédérale de Lausanne, Switzerland

Keywords: InAlN, GaN, VCSEL.

Over the past decade, III-nitride semiconductors have proven to be of the highest interest for optoelectronic applications in the short-wavelength range. White, blue and green light emitting diodes as well as violet and blue laser diodes are nowadays used in both mass consumer products such as domestic solid-state lighting sources or outdoor displays. More sophisticated devices like electrically-driven vertical cavity surface emitting lasers (VCSELs) have also been recently demonstrated.[1,2] VCSELs are well-known to offer several advantages compared to conventional edge-emitting lasers, e.g. single longitudinal mode, low threshold current density, circular emission beam and the possibility to process them easily into arrays of devices.
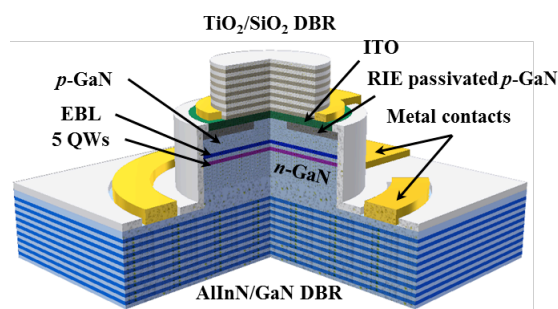
Figure 1. Scheme of our blue InAlN-based VCSELs.

Nevertheless, blue VCSELs still suffer from many issues, like challenging current injection schemes and lack of suitable distributed Bragg reflector (DBR) system. Either we face defective AlGaN/GaN DBRs or implement bottom dielectric DBRs that require challenging processing steps. In this context, the use of a bottom lattice-matched InAlN/GaN DBR[3] grown on a free-standing (FS) GaN substrate would allow improving device lifetime and thermal management while keeping the process flow simple.
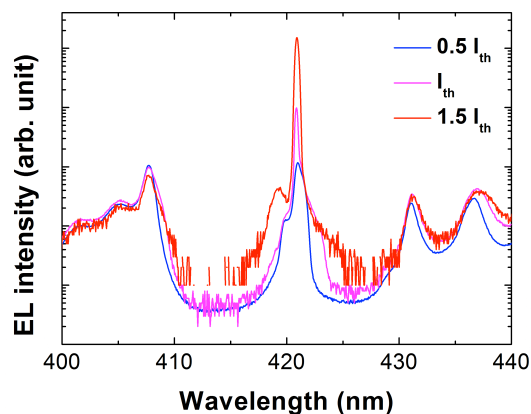

Figure 2. Electroluminescence (EL) spectra measured on a VCSEL for different (pulsed) currents ranging from below to above lasing threshold.

In this paper, we report on blue electrically-driven VCSELs grown on *c*-plane FS GaN substrates based on such an InAlN/GaN bottom DBR[4]. Some of the main limiting factors toward efficient blue VCSELs are discussed, and our strategies to overcome such drawbacks are described. Subsequently, our latest results on those devices are reported.

References

1. Y. Higuchi, K. Omae, H. Matsumura, and T. Mukai, *Appl. Phys. Express* **1**, 121102 (2008).
2. T.-C. Lu, S.-W. Chen, T.-T. Wu, P.-M. Tu, C.-K. Chen, C.-H. Chen, Z.-Y. Li, H.-C. Kuo, and S.-C. Wang, *Appl. Phys. Lett.* **97**, 071114 (2010).
3. J.-F. Carlin and M. Ilegems, *Appl. Phys. Lett.* **83**, 668 (2003).
4. G. Cosendey, A. Castiglia, G. Rossbach, J.-F. Carlin, and N. Grandjean, *Appl. Phys. Lett.* **101**, 151113 (2012).

Industry

Session chair : Tony Weidberg

VCSEL For Space Systems

A. Rissons, S. Poulenard and S. Bai

Institut Supérieur de l'Aéronautique et de l'Espace, Université de Toulouse, FRANCE

Keywords: VCSEL model, free space optical link, orbital systems.

For more than ten years, the Vertical-Cavity Surface Emitting Laser (VCSEL) became a key component for digital communications (Gigabit Ethernet). Indeed, the VCSEL performance and its assess have led the growth of the VCSEL market in the low cost short distance transmission links. As the VCSEL has been designed to achieve the requirements of the optoelectronic circuit planarization, its structure makes the VCSEL the smallest commercial available semiconductor laser diode (LD) type. Its small footprint, low electrical consumption and low thermal variation (wavelength, threshold current) allow the development of optical interconnects for harsh environment such as avionic, space, submarine. In addition, thanks to its low divergence and low linewidth, the VCSEL is an attractive candidate for high throughput Earth-Satellites multiplexed optical links. If the VCSEL emerged as key component for the digital optical transceiver, it didn't succeed to make a breakthrough in the microwave photonics applications were the Distributed Feedback (DFB) laser diode are in the lead[1]. However, the improvement achieved thanks to the advance of the VCSEL technology, especially for 1.3 and 1.55μm VCSEL, are promising for the microwave photonics applications. Today, an available 1.3 and 1.55 μm VCSEL provides a linewidth of 1 to 10MHz and a relative intensity noise (RIN) of -150dB/Hz[2]. With this performance, the introduction of the VCSEL on an optoelectronic oscillator (VBO: VCSEL-Based optoelectronic Oscillator) or let us expect to generate a stable microwave signal with low phase noise[3]. Another way to generate the microwave signal or a frequency comb is to put two VCSEL in Master-Follower configuration to make a VCSEL-by-VCSEL optical injection locking system (VOILS)[4].

By taking into account the cost effectiveness, the low size and low electrical consumption of the VCSEL, the VBO and VOILS are excellent candidates for the communication subsystems in satellite, probe or rover (such as Curiosity). Before the design of a demonstrator for space system payload, a modeling and characterization procedures in various operating modes are required in order to avoid an inadequate utilization of the VCSEL. It can be completed by modeling the steady state, small signal, large signal and noise, and by measurements of the optical spectrum, light-voltage-current, scattering parameters and relative intensity noise with a special attention to the space environment constraints such as thermal ambiance, electromagnetic compatibility, cosmic radiation, accelerations, chocks, vibration. Moreover, according to the space environment constraints, the qualification process, more strict than a land-based system, required reliable and robust device.

Today, some space industrials and agency announce their interest for the 1.3 and 1.55μm VCSEL and VECSEL for telecommunication[5]. Various systems will be explored. The objective is to find a trade-off between the best VCSEL performance and the effectiveness and robustness of the system in order to plan a launch in 2020.

References

1. H.Hellati, et al., TDA Progress Report, 42-128(1997)
2. A. Bacou, et al. , *IEEE J. Of Quantum Elec.,* **46, 3** (2010).
3 A. Rissons, et al. , IEEE International Topical on Microwave Photonics (2011).
4. . A. Hayat, et al., *IEEE Trans. On Microwave Theory and Techniques* (2009)
5. A. Rissons, et al. , IEEE International Topical on Microwave Photonics (2012).

Hermetic packaging of a twelve-channel
high bit rate VCSEL based transceiver

Vincent LECOCQ[1], Stéphane DENET[1], Caroline LYSZYK[1], Nadia WAZAD[2] and David VEYRIE[3]

[1] *Innoptics SAS, Talence, France, vlecocq@innoptics.com* [2] *Astrium, Elancourt, France* [3] *CNES, Toulouse, France*

Keywords: VCSEL, VCSEL Array, Ceramic Package, Hermetic, Parallel Optics, 10Gbps, Transceiver, Transmitter

High throughput data transmission encounters a growing demand in many applications today. Supercomputing and data centers have been driving new developments these past years, leading to the commercial availability of parallel optics transceivers and optical cables. These components allow tremendous benefits in terms of bit rate, lightness, power consumption, space saving… These features are highly valuable considering space applications as well, where copper based intra-satellite communication is becoming more and more complex.

In the scope of a Research and Technology program supported by CNES, and in partnership with EADS Astrium, Innoptics developed twelve-channel transmitter (based on VCSEL arrays) and receiver modules designed to meet the severe environmental specifications of space applications.

The main challenge of such a product is to achieve the hermetic packaging of arrays of emitters (or receivers). Existing solutions consist in hermetic feedthrough of the fiber, but mainly for single channel. However, this is very difficult to achieve with multiple fibers.
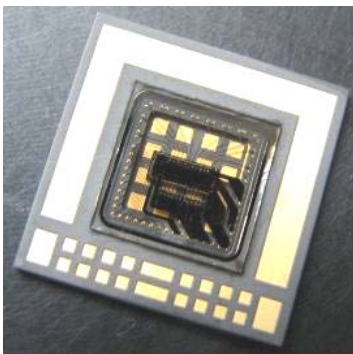

Figure 1. Hermetic "substrate
on ceramic package" subassembly

The concept that was implemented relies on the optical emission through a transparent substrate, the latter ensuring the following functions:
- Hermeticity of the package thanks to a solder seal ring on a ceramic package
- Optical window
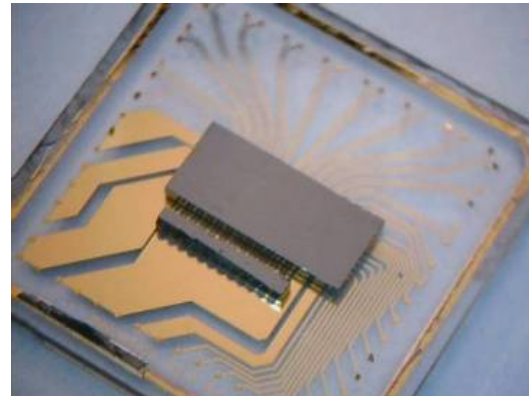- Electrical connection of the optoelectronic die

Figure 2. 12-channel driver and VCSEL array
on a transparent interconnection substrate

Thanks to a flip chip assembly process, the distance between VCSEL array (or photodiode array) and driver (or amplifier) can be minimized, allowing optimized signal integrity. RF lines are then routed through the ceramic package to a LGA type electrical interface.
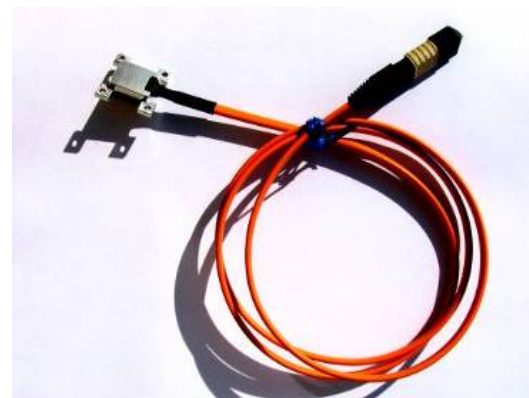

Figure 3. Pigtailed 12x transmitter

Light coming out of the window is coupled into a 50/125 fiber ribbon terminated by a twelve-channel MPO connector.

Recent Progress of InP-based Long-Wavelength VCSELs for Communications Applications

M. Ortsiefer, B. Kögel, J. Rosskopf, M. Görblich, Y. Xu, C. Gréus, and C. Neumeyr

Vertilas GmbH, Lichtenbergstr. 8, D-85748 Garching, Germany

Keywords: optical communication, InP, tunnel junction

The availability of high performance, cost effective and low power consumption light sources is regarded as an indispensable precondition for future generations of optical communication systems. Long-wavelength VCSELs are key components to fulfill these requirements. In our presentation we review the latest developments on InP-based buried tunnel junction (BTJ) VCSELs from laser performance to novel results in system applications.
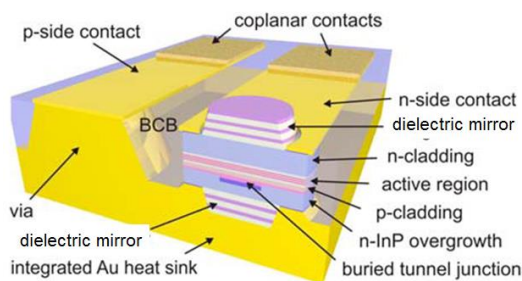
Fig.1 Schematic cross section of SC-VCSEL

To improve the modulation capability towards 25-40 Gbit/s we optimized both the inherent laser characteristics such as photon lifetime and the *RC*-limitations. By replacing the semiconductor output DBR with a large penetration depth for the optical field and consequently large photon lifetime with a high index difference dielectric DBR, the photon lifetime could be reduced by 40%. From our measurements on such short cavity (SC) VCSELs at 1.3 µm wavelength and 20°C as shown in Fig.2 we derive a possible intrinsic bandwidth of 25.4 GHz which would be sufficient for digital modulation at 40 Gbit/s. The actual bandwidth is still limited by parasitic capacitances including e.g. contact pads and depletion regions at the regrowth interface. Owing to the reduced damping, the SC-VCSELs have a maximum modulation of f_{3dB} = 15 GHz, which in the present devices is limited by the parasitic bandwidth of around 9 GHz. The D-factor D = 3.96 GHz/mA$^{0.5}$ is the rate at which the resonance frequency increases with bias current.

The VCSELs as shown in Fig. 1 additionally feature a coplanar contacting scheme for flip chip bonding and a common anode. Single emitter chips or arrays of well defined size can be separated from the wafer.
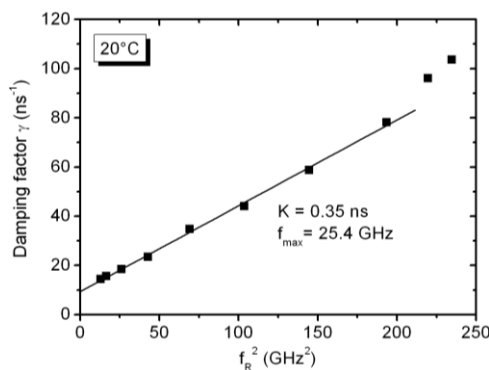

Fig.2 Damping factor vs. resonance frequency

For digital modulation the DC bias is superimposed with a non-return-to-zero (NRZ) bit sequence at 25 Gbit/s data rate and the eye diagram is recorded with a high-speed photo receiver and a sampling oscilloscope. The optical eye has an extinction ratio of 4.5dB and fits the 100 Gigabit Ethernet mask (100GBASE-LR4).
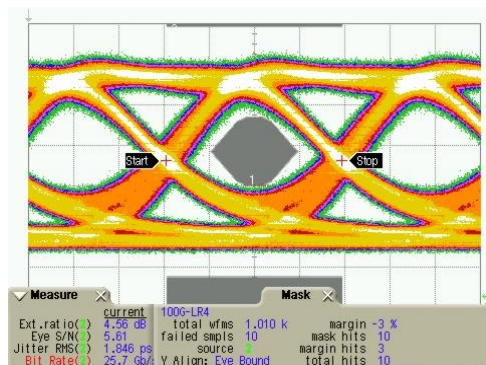

Fig. 3 Optical eye diagram of SC-VCSEL at 25Gbits/s data rate at 20°C

In addition, we will also present recent experiments with our VCSELs partly using advanced modulation formats for high speed and long range transmission.

References

1. R. Rodes et al., Journal of Lightwave Technology **31**, 689 (2013).
2. M. Müller et al., *Electron. Lett.* **48**,1487 (2012).
3. K. Prince *et al.*, *J. Optical Communications and Networkin.* **3**, 399 (2011).
4. T. Gibbon et al. , OFC, JThA30, (2010).

Progress and challenges in industrial fabrication of wafer-fused VCSELs

V. Iakovlev* [1,2] , A. Sirbu [1,2], Z. Mickovic [1], D. Ellafi [1], G. Suruceanu [2], A. Mereuta [2], A. Caliman [2] and E. Kapon [1] ,[2]

[1] *Laboratoire de Physique des Nanostructures, Ecole Polytechnique Fédérale de Lausanne, Switzerland*
[3] *BeamExpress S.A., Lausanne, Switzerland*

Keywords: Green photonics, wafer fusion, long wavelength VCSELs, industrial fabrication.

The effort for the industrialization of wafer-fused, long wavelength (LW) vertical cavity surface emitting lasers (VCSELs) for wavelength division multiplexing (WDM) optical fiber communication applications has a significant history. Back in 2005 we have demonstrated the compliance of the overall performance of wafer-fused VCSELs with the requirements of the 10 GBASE-LX4 IEEE.802.3ae standard [1]. The devices were fabricated out of 2-inch VCSEL wafers produced at BeamExpress by a proprietary wafer fusion technique, also termed "localized wafer fusion". Localized fusion helps to regulate the fusion process across the wafer, yielding high-quality fused interfaces with high uniformity and repeatability. The good quality of the double fused-wafer is allowing the application of standard VCSEL processing technology. The subsequent processing steps include reactive ion etching through the top distributed Bragg reflectors (DBRs) down to the top intra cavity contact layer, selective chemical etching through the active cavity, stopped at the bottom intra-cavity contact layer, passivation of the p-n junction and deposition of ohmic contacts on both intra-cavity contact layers. Despite the complex device structure and processing, it is possible to achieve high uniformity and good control of important device parameters. For example, the measured average cavity length over the entire double-fused 2-in VCSEL wafer (excluding 5-mm-wide margins) exhibits a standard deviation of less than 2 nm, which reflects a good thickness uniformity of both the active cavity layers and the DBRs. Back in 2005, single-mode emission power in excess of 1.2 mW was been demonstrated in the temperature range of 20-80°C at operating voltage below 2.5 V. Single-mode emission with 40-dB side mode suppression ratio as well as 3.2-Gb/s modulation capability was demonstrated with these devices . It is important to note that the progress in 1300 nm wavelength wafer-fused VCSELs was backed by the progress in 1500 nm wafer-fused VCSELs ,As of today, 40GBase-LR4 (4x10-Gbps) optical transceivers in QSFP+ modules using uncooled distributed feedback (DFB) lasers are already on the market, with power dissipation specified at 3.5 W. For next-generation 40GBase-LR4, the use of single mode VCSELs and low power consuming VCSEL drivers may result in more than 40% power consumption savings, reducing 40-GbE optical transceiver power dissipation significantly below today's 3.5-W barrier. Owing to their inherent low power consumption, long wavelength VCSELs are finally positioned to revolutionize intermediate-reach transmission (>1km), just as 850nm VCSELs revolutionized use of multi-mode fiber. As long wavelength VCSELs are come of age, a good maturity check for their technology is now its capability to meet requirements of building 4x10 Gbps CWDM transmitter modules emitting at 1271, 1291, 1311 and 1331 nm with reduced power consumption. Three main approaches for the fabrication of LW-VCSELs have emerged: undercut quantum well , buried tunnel junction and regrown tunnel junction [2] . However, there have not been reports on the industrialization and reliability of the two former methods. In this paper, we demonstrate that regrown tunnel junction, wafer-fused VCSELs emitting in the 1310 nm band for 10 Gbps CWDM applications have now reached maturity for industrial fabrication in high volume. The challenges for increasing operation speeds and production volumes will also be highlighted [3].
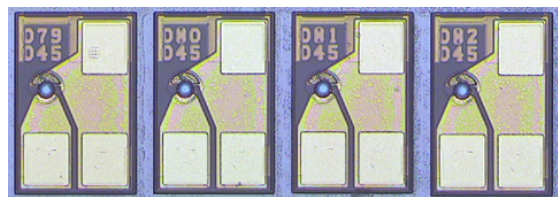
Optical microscope picture of industrially fabricated long wavelength wafer fused VCSELs on GaAs substrate

Reference

1.V. Iakovlev, et all. EEE Photonics Technology Letters, vol. 17, p. 947-949, (2005).
2.E. Kapon and A. Sirbu, Nature Photonics, vol. 3, p. 27-29, (2009).
3.V. Iakovlev, et al. Photonics West 2013, Vertical-Cavity Surface-Emitting Lasers XVII, San Francisco, California, USA, 2013.

High Power VCSEL Systems

U. Weichmann*, P. Gerlach, S. Gronenborn, Xi Gu, G. Heusler, R. Jaeger, J. Kolb, M. Miller, H. Moench,
P. Pekarski, J. Pollmann-Retsch, A. Pruijmboom

*Philips Photonics Aachen, Steinbachstraße 15, D-52074 Aachen, Germany, ulrich.weichmann@philips.com

Keywords: VCSEL arrays, high power.

Systems with arrays of VCSELs can reach optical output powers in the range of many kilowatts and provide a robust and economic solution for many applications with low to moderate brightness requirements[1,2]. Such applications are illumination, heating, thermal processing and solid-state laser pumping. The use of VCSEL arrays for high power laser diode applications enables multiple benefits: Full wafer level production of VCSELs including the combination with micro-optics; assembly technologies very similar to LED assembly thus profiting from the rapid development in solid state lighting; an outstanding reliability and a modular approach on all levels. Due to these advantages high power VCSEL systems will become a new alternative to classical high power diode laser systems.
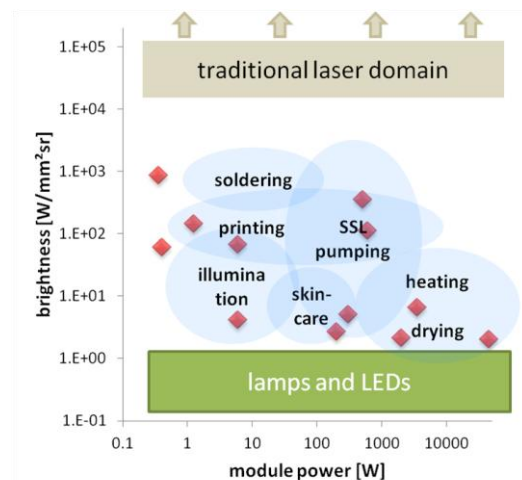

Figure 1: Application space of High Power VCSEL Systems. The red diamonds indicate output power and brightness of actual prototypes realized by Philips Photonics.

The application space for High Power VCSEL Systems is defined by the brightness of the VCSEL itself and lies in between the domains of classical laser applications and those served by lamps or LEDs. This is shown in Figure **1**, where typical applications areas as well as actual prototypes realized by Philips Photonics are indicated.

To realize high power arrays with power levels of several 10 kW, a modular approach is used: Arrays of VCSELs are soldered to AlN-submounts that insulate the arrays from the water-cooled heat sink and enable the electrical connection between the VCSEL arrays. Micro-channel coolers are chosen as the heat sink and several submounts are mounted on the cooler. The number of arrays per submount and the number of submount per cooler is adjusted to the needs of the specific application. Each cooler forms one so-called sub-module with an output power of about 500W. Such a cooler is shown in the left picture of Figure 2. Several of these sub-modules are assembled on a line to form a high power system with output powers in the kW-range.
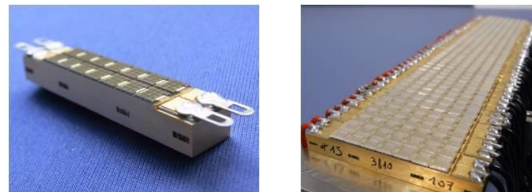

Figure 2: Cooler assembled with VCSEL arrays on sub-mounts (left) and the mounting of these building blocks into a long line (right).

The different applications mentioned in Figure 1 have different requirements for the intensity distribution on the work-piece. Heating and drying for example requires an area illumination with a low brightness and intensity of only 1W/mm². This can be realized by simply using the radiation emitted directly from the high power system. Placing macroscopic optics in front of the system allows to tailor the intensity distribution on the workpiece to realize for example a line focus and increase the intensity to 10W/mm². With additional microoptics on the VCSEL-arrays, a spot with an already intermediate intensity of 100W/mm² useful for solid-state laser pumping is realized.

References

1. J. F. Seurin et al., High-power high-efficiency 2D VCSEL arrays, *Proc. of SPIE* **6908** (2008).
2. H. Moench et al., High power VCSEL systems for tailored intensity distributions, *Proc. of SPIE* **7952** (2011)

Miniature low-cost Platform for Volume Applications in VCSEL-based Gas Sensing

R. Strzoda, A. Popescu, A. Hartmann, M. Fleischer

Siemens AG, Corporate Technology, Otto-Hahn-Ring 6, 81739 München, Germany

Keywords: TDLS, gas sensor.

Although gas sensing devices based on Tunable Diode Laser Spectroscopy (TDLS) offer many outstanding advantages in terms of achievable accuracies, selectivity, robustness and long term stability, they are settled only within specialized applications with a volume in the order of 1000 units per year worldwide. However, many more potential applications with quantities of $>10^5$/year like eg. air quality monitoring would profit from this technique as soon as cost effective systems are available. Promising candidates are systems for H_2O, O_2 or CO_2 monitoring.

For cost reduction an adjustment-free optical cell and highly integrated electronics with a powerful processor are mandatory.

The diffuse reflective design of the optical cell (see Fig. 1) supports the low cost idea in two ways. It is free of fine-adjustment and if it is used to measure gas inside a chamber, it can be attached as a single complete block requiring only one opening in the wall.

The detection scheme is based on Wavelength Modulation Spectroscopy (WMS). In WMS the spectra are recorded by tuning the wavelength of the laser using current-ramps superimposed with a small signal sine modulation. Usually the 2nd harmonic of the modulation signal is evaluated to extract the gas concentration. This concept is widely used as it is easily realized by lock-in techniques.
The evolution of the electronics ranges from the analog lab design using discrete lock-in amplifiers, PC's equipped with data acquisition cards, stand alone electronics[1] without and with FPGA for certain functions to the 'single chip' design presented today.

The sensor consists of the laser driver with the modulation signal generation, a temperature stabilization stage and a receiver, which is realized by a photo diode and a transimpedance amplifier; a gain adjustment stage, an AD-converter and the digital demodulator follow. The digitized spectra are evaluated in real-time on the processor with different degrees of complexity from maximum tracking to nonlinear curve fitting of spectral models. The presented design includes also a power

supply and data communication. The core functionalities are realized on a single chip by a mixed signal microcontroller of the latest generation enabling significantly reduced hardware costs.

Figure 1 shows a picture of the realized hardware of a CO_2 sensor. It can be used as air quality monitor in HVAC applications. First results deliver a resolution of 50 ppm at 1 s response time (see Fig. 2).
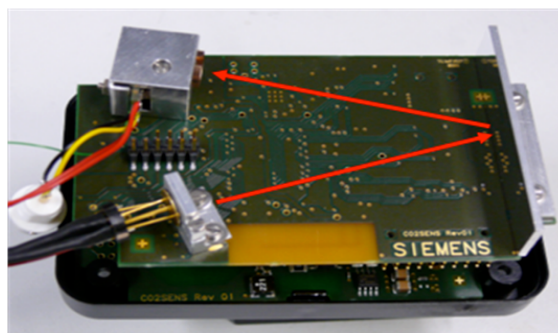

Figure 1: CO_2-sensor setup with a form factor of a conventional power supply (overall length: 110 mm). The optical path is indicated on the back of the PCB.
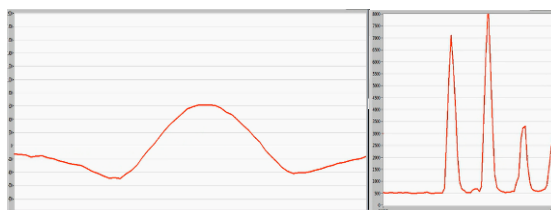

Figure 2: CO_2-sensor operation. Left: Measured 2f-WMS spectrum; Right: Temporal evolution of the ambient CO_2-concentrations; the time scale ranges from 0 to 80 s and the conc. scale from 0 to 8000 ppm.

References

1. Chen, J.; Hangauer, A.; Strzoda, R.; Amann, M.-C., "VCSEL-based calibration-free carbon monoxide sensor at 2.3 µm with in-line reference cell", Applied Physics B: Lasers & Optics(2011), vol. 102 Issue 2 p. 381-389.

SWIFTS TECHNOLOGY: A NEW TOOL FOR VCSEL SPECTRUM ANALYSIS

Christophe Bonneville[1], Etienne Le Coarer[2], Pierre Benech[3], Thierry Gonthiez[1], Fabrice Thomas[1], Bruno Martin[1], Renaud Puget[1], Eric Morino[1]

1 Resolution Spectra Systems, 38240 Meylan, France
2 Université Joseph Fourier, 38041 Grenoble, France
3 IMEP-LAHC, Minatec, 38016 Grenoble, France

Keywords: Spectrum, Measurement, Mode Hopping, Spectral Width, Mode Partition Ratio, Spectral Density, SWIFTS.

VCSELs are subject to multimode wide spectral shape, mode hopping, strong sensitivity to the operating point, temporal instability and inhomogeneity in production. At the same time, demanding applications such as optical link and instrumentation require strong spectral specification.
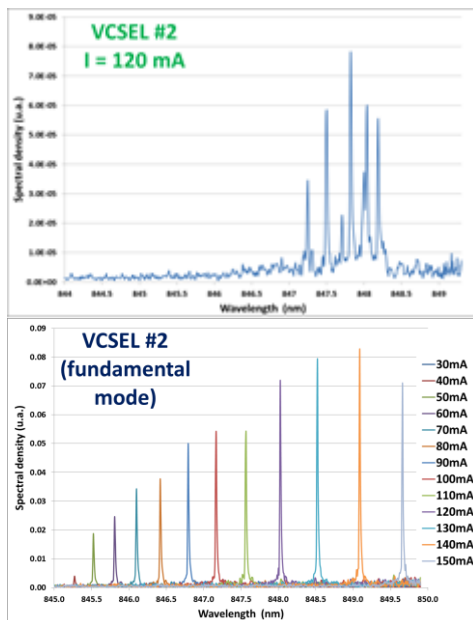
Fig. 1: 850 nm VCSEL spectrum (left) monitored during current scan mapping (right).

In this talk we will present how SWIFTS – Stationary-Wave Integrated Fourier Transform Spectrometer – technology opens up new opportunities in VCSEL spectrum analysis. Systems based on this technology can typically achieve spectral resolution of few GHz / pm with a good SNR over a bandwidth from several nm to few hundred nm and a high frame rate of tens of kHz on a few mm² chip. To demonstrate how SWIFTS principle can be a powerful tool for VCSEL analysis and control, we will explain the principle of this patented technology and present results on VCSEL in VIS-NIR range. Both high spectral resolution and high measurement rate together provide new possibilities in VCSEL spectrum analysis which can't be achieved by OSA: resolving all modes with an absolute accuracy of 0.001 nm, precise study of the temporal instability and mode partition ratio, very fast highly sampled current or temperature mapping including wavelength and relative optical power of each mode.

The current development in terms of hardware and signal processing of such instrument will be presented and we will share our views about how to address more accurately again VCSEL testing with SWIFTS technology.

References

1. le Coarer, E., Blaize, S., Benech, P., Stefanon, I., Morand, A., Le Rondel, G., Leblond, G., Kern, P., Fedeli, J.-M., Royer, P., Nature Photonics, 1, 8, 473 – 478, (2007)
2. Knipp, D., "Nanophotonics: Spectrometers shrink down", Nature Photonics 1, 8, 444–445 (2007)
3. C. Bonneville; F. Thomas; M. de Mengin Poirier; E. P. Le Coarer; P. Benech; T. Gonthiez; A. Morand; O. Coutant; E. Morino; R. Puget; B. Martin, SPIE 8616-20, (2013)
4. Lippmann, G. Compte Rendus de l'Académie des Sciences (Paris) 112, 274–275 (1891)
5. Lippmann, G. Compte Rendus de l'Académie des Sciences (Paris) 92-102 (1894).
6. Patent n° WO 2006064134 (A1), (Date of Publication : 2006-6-22), Pierre Benech/ Etienne Le Coarer
7. Patent n° WO 2007017588 (A1), (date of publication : 2007-02-15)

Telecom/Datacom

Session chair : Åsa Haglund

Progress Toward 50Gb/s-Km VCSEL Operation

Meng Peun Tan[1], James A. Lott[2,3], Nikolay N. Ledentsov[2], Dieter Bimber[3], and **Kent D. Choquette**[1]

[1]*University of Illinos at Urbana–Champaign, Urbana, Illinois 61801   USA*
[2]*VI Systems, GmbH, Berlin, D-10623, Germany*
[3]*Technische Universität Berlin, Berlin D-10623, Germany*

Keywords: Large signal modulation, bandwidth-distance product, vertical cavity lasers

Vertical-cavity surface-emitting lasers (VCSELs) combined with multimode fibers have been widely used in short-haul data optical data communication due to low power consumption and low cost. Transmission distance at high data rate is expected to increase with reduced chromatic dispersion if the laser source has narrow spectral width [1]. The bandwidth-distance product of data communication VCSELs has grown from 12 to 25 Gb/s/km recently [2-4]. In this work we describe the advantages of using a photonic crystal VCSEL with separated optical and current aperture to create high modulation speed single mode emission.
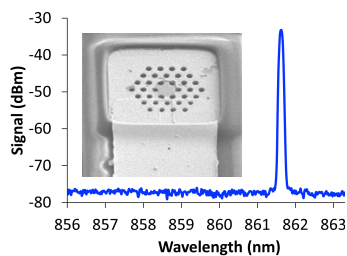

Fig. 1: Single mode optical spectrum (inset) image of photonic crystal VCSEL.

The photonic crystal design parameters determined by photolithography are hole pitch, *a* and hole diameter, *b*. Proton implantation is employed for current confinement. Various photonic crystal designs and optical aperture sizes yield single mode waveguide condition [5], whereas the implant aperture has to be sufficiently small to reduce diffusion capacitance [6] and threshold current. Fig. 1 shows the VCSELs operate in the fundamental mode with an intensity more than 40 dB above the noise floor and no higher order modes are visible. A SEM image of a completed device after polyimide planarization is shown in Fig. 1 inset.

Small signal modulation measurements have yielded 3dB bandwidth of 18.3 GHz at operation current density less than 10 kA/cm^2. Large signal modulation at up to 30 Gb/s back-to-back has also been achieved. Bit error rate plots for the photonic crystal VCSEL are shown in Figs. 2(a) and (b) using

a nonreturn to zero data pattern with a $2^7 - 1$ pseudorandom binary sequence. The peak-to-peak modulation amplitude is 0.5 V and the VCSEL is biased at 5.9 mA at room temperature. Using Draka OM3+ fiber, error free transmission at link lengths up to 1 km have been acheived. As evident in Fig. 2 (b), BER of 10^{-12} is achieved at an operating current density of 5.4 kA/cm^2, which is about half of the industrial benchmark for long lifetime operation [3]. Further improvement of the bandwidth-distance product will require higher output power.
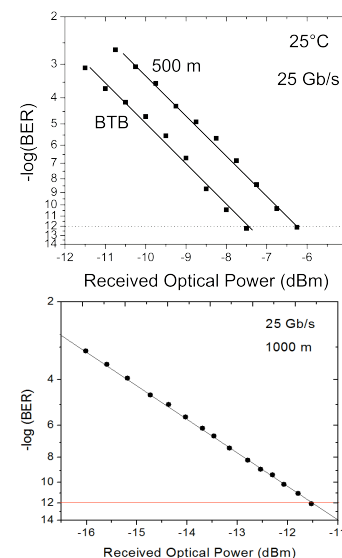

Fig. 1: Bit-error-rate versus received power for (a) back-to-back and 500 m of fiber; and (b) 1km of fiber.

References

[1] R. E. Freund, C.-A. Bunge, N. N. Ledentsov, D. Molin, and Ch. Caspar, *J. Light. Tech.*, **28**, 4 (2010).
[2] E. Haglund, Å. Haglund, P. Westbergh, J.S. Gustavsson, B. Kögel and A. Larsson, *Elect. Lett.*, **48**, 9 (2012).
[3] B. M. Hawkins, R. A. Hawthorne III, J. K. Guenter, J. A. Tatum, and J. R. Biard, *Proc. 52nd Electron. Comp. Technol. Conf.* (2002).
[4] P. Moser, J. Lott, P. Wolf, G. Larisch, A. Payusov, N. Ledentsov, W. Hofmann, and D. Bimberg, *IEEE Phot. Tech. Lett.*, **24**, 1 (2012).
[5] M. P. Tan, J. A. Lott, N. N. Ledentsov, D. Bimberg, and K. D. Choquette, submitted to *IEEE Phot. Tech. Lett.* (2013).

850 nm datacom VCSELs for higher-speed and longer-reach transmission

E. Haglund, P. Westbergh, E. P. Haglund, R. Safaisini, J. S. Gustavsson, K. Szczerba, Å. Haglund and A. Larsson

Department of Microtechnology and Nanoscience (MC2), Photonics Laboratory, Chalmers University of Technology, Göteborg, Sweden

Keywords: datacom, high-speed, quasi-single mode, bandwidth.

The 850 nm GaAs-based VCSEL is already the dominating technology for transmitters in optical interconnects up to 100 m in datacenters, thanks to low-cost fabrication, excellent high-speed properties at low currents and the existence of high-speed OM4 multimode fiber optimized for this particular wavelength. Future datacenters will require faster and more energy-efficient VCSELs to increase the overall bandwidth and reduce the power consumption of the datacenter network. In addition, longer-reach interconnects exceeding 1 km will also be required as datacenters grow into large multi-building complexes.

By optimizing the doping profiles of the DBRs to reduce resistance, using a short (½-λ) cavity to improve longitudinal optical confinement and optimizing the photon lifetime for optimal damping, we obtained a record-high small-signal modulation bandwidth of 28 GHz for a ~4 µm oxide aperture VCSEL. A 7 µm oxide aperture VCSEL (~27 GHz bandwidth) enabled error-free transmission (bit-error-rate $< 10^{-12}$) at 47 Gbit/s back-to-back (BTB) and 44 Gbit/s over 50 m of OM4 fiber, using a VI-systems R40-850 photoreceiver (30 GHz) with an integrated limiting transimpedance amplifier. The high bandwidth also allows for error-free transmission at 40 Gbit/s BTB at 85°C [1]. By instead using a New Focus 1484-A-50 photoreceiver (22 GHz) with a linear amplifier, 50 Gbit/s error-free transmission was achieved BTB at room temperature, see figure 1.

At longer transmission distances (> 300 m), the large spectral width of VCSELs leads to severe signal degradation by fiber dispersion. We have investigated two methods of fabricating low-spectral width quasi-single mode VCSELs to mitigate this problem. By using a small oxide aperture of ~3 µm, error-free transmission was achieved at 22 Gbit/s over 1.1 km of OM4 fiber [2]. An alternative approach is to use an integrated mode filter in the form of a shallow surface relief to reduce the spectral width of the VCSEL. The mode filter allows for the use of a larger oxide aperture and thereby enables a lower resistance and operation at a lower current density. A 5 µm oxide aperture VCSEL with a mode filter enabled error-free transmission at 25 Gbit/s over 500 m of OM4 fiber [3].
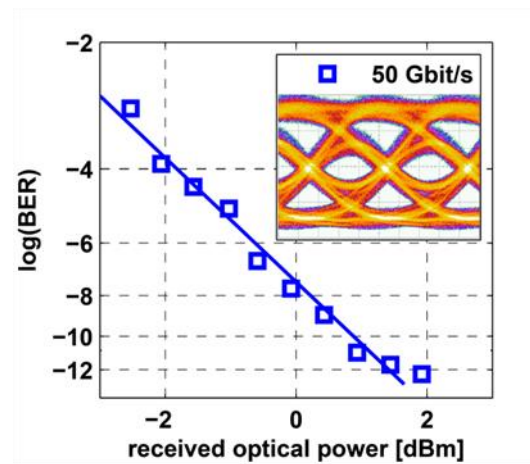

Figure 1. BER vs. received optical power at 50 Gbit/s BTB with eye diagram.

References

1. Westbergh, P., et al.: 'High-Speed Oxide Confined 850-nm VCSELs Operating Error-Free at 40 Gb/s up to 85 °C', *IEEE Photon. Technol. Lett.*, 2013, **25**, (8), pp. 768-771
2. Safaisini, R., et al.: '20 Gbit/s error-free operation of 850 nm oxide-confined VCSELs beyond 1 km of multimode fibre', *Electron. Lett.*, 2012, **48**, (19), pp. 1225-1227
3. Haglund, E., et al.: '25 Gbit/s transmission over 500 m multimode fibre using 850 nm VCSEL with integrated mode filter', *Electron. Lett.*, 2012, **48**, (9), pp. 517-519

Epitaxial-Stacked Double-Active Region in InP-based 1.55 μm Short-Cavity VCSELs for High-Speed Data Transmission

Silvia Spiga, Alexander Andrejew, Michael Müller, Markus-Christian Amann

Walter Schottky Institut, Technische Universität München, Am Coulombwall 4, 85748 Garching, Germany

Keywords: VCSEL, energy-efficiency, InP.

In the past two decades, cost-effective and energy-efficient optical interconnection for access- and metropolitan- networks has driven the datacom- and telecom- applications development. Vertical cavity surface emitting laser (VCSEL) emitting in the optical C-band have been demonstrated to be suitable for this purpose, and error free data transmission of 25 Gb/s over 4.2 km was demonstrated for a Short-Cavity VCSEL (SC-VCSEL) with small-signal modulation bandwidth (υ_{3dB}) in excess of 17 GHz[1]. Furthermore, higher data rate of 40 Gb/s could be reached in back-to-back configuration for VCSEL with υ_{3dB} of 19 GHz[2]. However, the exponential growth of the network traffic goes hand in hand with the demand for reducing the price for transported information. This motivates the further optimization of the already existing VCSELs, requiring higher efficiency of the device and lower power dissipation, as well as high modulation bandwidth. A further step in this direction can be achieved by implementing the stacked active region (AR) design[3]. Unlike the monolithic active region arrangement[1], the novel design consists of multiple ARs placed in series at different maxima of the optical field along the laser cavity.

In this work, we will present a InP-based SC-VCSEL with epitaxially-staked double-active-region emitting at 1.55 µm. As shown schematically in Figure 1, two identical ARs, containing 3 quantum wells each (2x3QWs), are embedded between a low
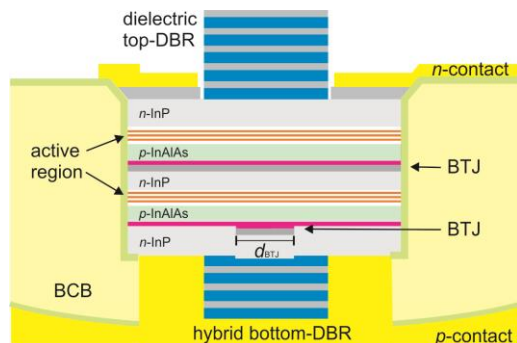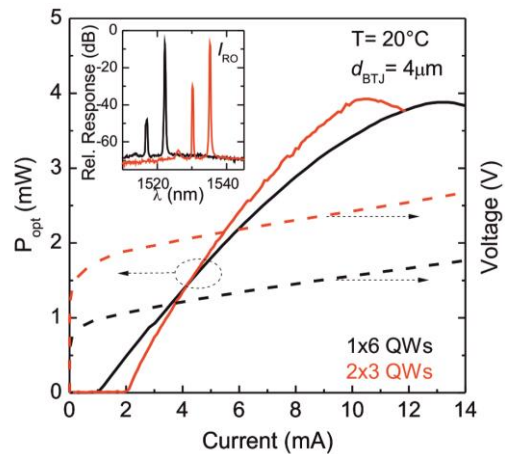

Figure 2. The power-current-voltage characteristics as a function of the DC-current are presented for devices with single (black lines) and stacked (red lines) active regions at room temperature operation. In the insert, the optical spectrum at roll-over current is given.

n-doped InP layer and a p-cladding. An unstructured p^{++}/n^{++} buried tunnel junction (BTJ) is placed between the two ARs, and, a second circularly shaped BTJ is structured on the bottom side of the laser to achieve current confinement. In order to reduce absorption losses and maximize the optical gain, the highly conducting junction layers and the two ARs are placed at the minima and maxima of the optical field, respectively. In this way, high differential quantum efficiency of 80% is achieved at room temperature, as shown in Figure 2. In addition, we will present the static and dynamic characteristics of a staked-AR VCSEL with 2x3QWs in comparison with a SC-VCSEL with 1x6QWs. Particularly, temperature dependence of the characteristic parameters (i.e threshold current, maximum power) and small-signal modulation analysis results will be discussed.

Figure 1. A schematic image of a SC-VCSEL with stacked double-active regions is shown (not to scale).

References

1. M. Müller et al., IEEE J. Sel. Top. Quantum Electronics **17**, 1158 (2011).
2. Hofmann et al., Electronics Letters **47**, 270 (2011).
3. Kim et al., Appl. Phys. Lett. **74**, 3251 (1999).

Impact of Cavity Photon Lifetime on High Speed performance of 1.3-µm Wavelength Wafer-Fused VCSELs

D. Ellafi[1], V. Iakovlev[1], A. Sirbu[1], G. Suruceanu[2], A. Caliman[2], A. Mereuta[2], Z. Mickovic[1] and E. Kapon[1,2]

[1] *Laboratory of Physics of Nanostructures, École Polytechnique Fédérale de Lausanne (EPFL), CH-1015 Lausanne, Switzerland*
[2] *BeamExpress S.A., 1015 Lausanne, Switzerland*
E-mail: dalila.ellafi@epfl.ch

Wafer fused long wavelength vertical cavity surface-emitting lasers (WF-LW-VCSELs) operating at 1310 nm are gradually establishing themselves as key components for uncooled, low power, long wavelength transceivers [1] for decreasing the total power consumption in big data centers (BDCs). In ref [2], it was demonstrated that photon lifetime has a significant impact on the modulation bandwidth of 850 nm multimode VCSELs.

In this paper, we demonstrate that photon lifetime reduction in WF-LW-VCSEL by post-growth reduction of the total number of the top DBR layers for increasing modulation performance at 10 Gbps data rates.

The investigated VCSEL devices were fabricated by the wafer fusion technique [3] from the batch described in [4] and have a total of 22.5 top DBR pairs. Selective etching was then applied on the top DBR to remove one pair to a number of selected VCSELs with the same design, all from this particular wafer.

Light–current (L-I), s21 and eye diagram measurements were performed at room temperature (RT) on the same devices, with 22.5 and 21.5 top DBR pairs (as grown and after etching). The electrical VCSEL parameters were not affected by the etching.

Reducing the number of top DBR pairs results in a penalty on the threshold current (increase from 0.7mA to 0.9mA) and in an increase of the maximum output power from 4.1mW to5.4mW (see Fig 1.a).The maximum f3dB increases from 5GHz to 6GHz at operating currents of 5mA and 6mA, respectively (Fig1.b). The 21.5 pairs VCSEL structure exhibits a photon lifetime τp of 6.6ps and K-factor of 0.51ns. For the 22.5 pairs VCSEL structure, the photon lifetime and the K-factor increase to 7ps and 0.62ns, respectively.

At RT, the 10.3Gb/s eye diagrams biased at 7mA (Fig1.c and d) are more open after one pair removal.

The presented results are in line with previous results [5] of an improvement of the modulation bandwidth by reducing the photon lifetime obtained by applying a shallow etching of the topmost DBR layer, allowing as well an extraction of the internal quantum efficiency of the device. Both studies provide means for tuning the high speed modulation characteristics of WF-LW-VCSELs by post-growth processing.

References

[1] V. Iakovlev *and al*., Proc. of SPIE Vertical-Cavity Surface-Emitting Lasers XVII, Vol. **8639**, 2013.

[2] P. Westbergh *and al.*, Electronics Letters, 2010 Vol. **46** No. 13, June 2010.

[3] V. Iakovlev *and al.*, Photonics Technology Letters, Vol. **17**, No. 5, pp. 947–949, May 2005.

[4] V. Iakovlev *and al.*, Lasers and electro-optics,CLEO, pp 1 – 2, 2007.

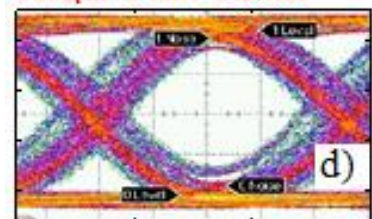[5] D. Ellafi *and al.*, to be presented at CLEO Europe 2013.
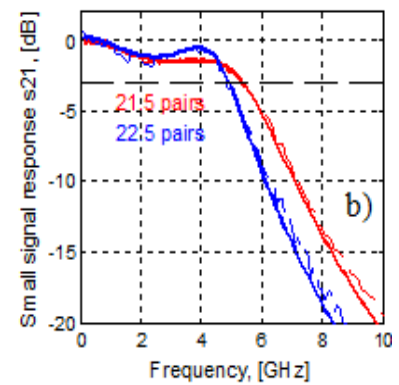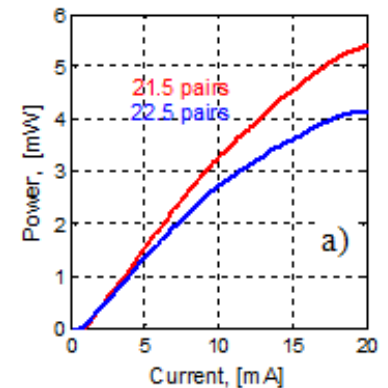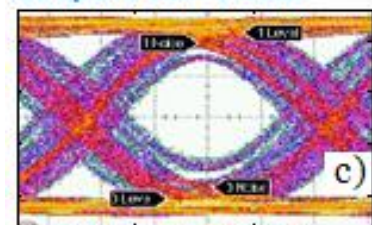
Fig1. (a) LIV at RT, (b) s21 response at RT, (c, d) Eye diagrams at 7mA, 0.53Vpp and 2^7-1 PRBS

Energy efficient 850 nm VCSELs for Data and Computer Communication

P. Moser, P. Wolf, G. Larisch, H. Li, J. A. Lott, and D. Bimberg[1]

Institut für Festkörperphysik und Zentrum für Nanophotonik, Technische Universität Berlin, Hardenbergstrasse 36, D-10623, Berlin, Federal Republic of Germany
[1]*also with the King Abdulaziz University, Jeddah, Kingdom of Saudi Arabia*

Keywords: vertical cavity surface emitting lasers (VCSELs), energy efficiency, multimode fiber, optical interconnects.

To date the maximum reported error-free bit rate (BR) of VCSELs operating at room temperature is 47 Gb/s[1] using multimode 850 nm VCSELs with oxide aperture diameters of 7-11 μm. We demonstrated[2] that VCSELs with oxide aperture diameters of ~4 μm or less emitting in a single or quasi single fundamental transverse mode are more energy efficient than VCSELs with larger oxide aperture diameters when operated at low bias above threshold. The intrinsically larger D-factors are then beneficial. We recently demonstrated 850 nm VCSELs operating error-free up to 40 Gb/s with only ~100 fJ dissipated energy per bit[3].

By employing such small oxide aperture diameter VCSELs we simultaneously achieve long transmission distance[4] across multimode fiber (MMF) at high BR and at record low dissipated energy per bit. Despite the small aperture diameters the current density (J) required for error-free operation is comparable to the J for VCSELs having larger aperture diameters[1,5].
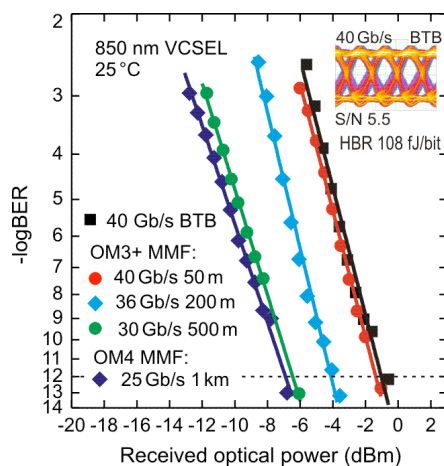

Figure 1. Bit error ratio (BER) versus received optical power at different bit rates and across different types and lengths of multimode optical fiber. Inset: optical eye diagram at 40 Gb/s.

Using 2^7-1 PRBS NRZ modulation error-free (BER < 1×10^{-12}) operation at 40, 36, 30, and 25 Gb/s

across 50, 200, 500, and 1000 m of MMF is achieved dissipating only 100 fJ/bit[4] at 25 Gb/s. In a back-to-back (BTB) configuration the dissipated energy is as low as 56, 85 and 108 fJ/bit at 25, 30 and 40 Gb/s, respectively. At 25 and 30 Gb/s across 1000 and 500 m of MMF the J is 20 kA/cm^2, only slightly larger than that of VCSELs with an additional mode filter[5] that achieve 25 Gb/s across 500 m MMF at 18 kA/cm^2. At 40 and 36 Gb/s J is approximately 25 kA/cm^2.
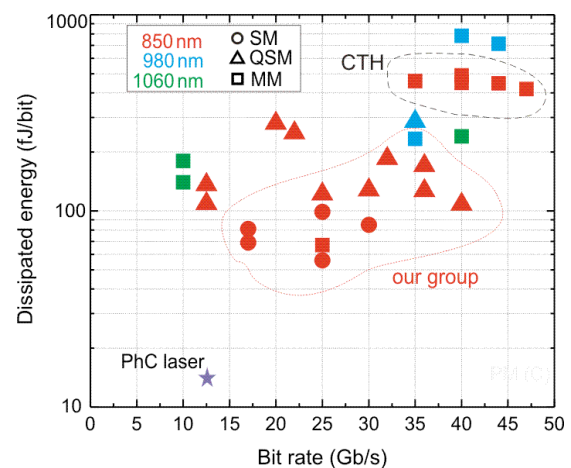

Figure 2. Dissipated heat energy per bit versus bit rate for single mode (SM), quasi single mode (QSM) and multimode (MM) VCSELs emitting at peak emission wavelengths of about 850, 980, and 1060 nm, all at room temperature. The value for a photonic crystal (PhC) laser showing open optical eye diagrams is indicated with a star.

References

1. P. Westbergh et al., *IEEE Photon. Technol. Lett.*, **25**, 768 (2013).
2. P. Moser et al., *Electron. Lett.* **48**, 1292 (2012).
3. P. Wolf et al., *Electron. Lett.* (2013), DOI: 10.1049/el.2013.0617 (accepted for publication).
4. P. Moser et al., *Proc. IEEE OI Conf. 2013*, Santa Fe, NM, USA, 5-8 May 2013, paper TuA4.
5. E. Haglund et al., *Electron. Lett.* **48,** 517 (2012)

Infrared VCSELs for Short Distance High Bit Rate Free Space Optical Interconnects

J. A. Lott, P. Moser, G. Larisch, V. Kalosha, H. Li, P. Wolf, and D. Bimberg[1]

Institut für Festkörperphysik und Zentrum für Nanophotonik, Technische Universität Berlin, Hardenbergstrasse 36, D-10623, Berlin, Federal Republic of Germany
[1]*also with the King Abdulaziz University, Jeddah, Kingdom of Saudi Arabia*

Keywords: vertical cavity surface emitting lasers (VCSELs), optical interconnects.

The idea of connecting displays, mobile telephones, televisions, computers, and other networked gadgets wirelessly at optical fiber bit rates is quite intriguing. In fact line-of-sight free space optical interconnects[1] across distances of zero (e.g. abutted light source and detector devices) up to a few meters based on infrared (~940 to 960 nm) vertical cavity surface emitting lasers (VCSELs)[2-4] and Si or group III-V photodiodes offer to us huge consumer and medical market opportunities. Other free space applications include handheld remote controls (replacing RF units), USB interfaces, gesture recognition, laser illumination, laser detection and ranging, and in (as 2D arrays to increase the pulsed or CW output power) a plethora of industrial tools[5].

The key component for short distance free space optical communications systems is the ubiquitous infrared VCSEL. In addition to energy efficient operation at high bit rates we seek higher than typical output powers per device without cooling, and designs that facilitate the simultaneous operation of an array of VCSELs to boost the output power for specific applications. In this work we detail our VCSEL designs and modal modeling results. We also present our first data transmission results based on our low output power (~10 mW per device) single fundamental transverse mode VCSELs designed for flip-bonding onto metalized silicon carriers for hybrid integration with driver, receiver, and optional processor integrated circuits.

We grow our VCSELs on GaAs substrates. A representative design consists of three to five InGaAs QWs with GaAsP barriers. The DBRs are composed of $Ga_{1-x}Al_xAs$ (e.g. x~0.12 and 0.9) with graded interfaces and spatially varying doping. The upper p-doped DBR has 28 to 32 periods including $Ga_{0.02}Al_{0.98}As$ oxide aperture layers. The lower DBR is divided into a 4 to 7 period n-doped (n)DBR, a 1.25λ-thick (n)GaAs intracavity ohmic contact layer, and a 12 to 16 period undoped DBR just above the substrate. We characterize devices via L-I-V and data transmission experiments using a standard set-up[6], including MMF, lenses, and variable free space distances. We also characterize prototype transceiver

optical subassemblies containing our flip-bonded VCSELs. We obtain a CW SM output power up to 15 mW (see Figure 1) and NRZ error free (BER < 1×10^{-12}) free space data transmission using a PRBS with 2^7-1 word length (see Figure 2).
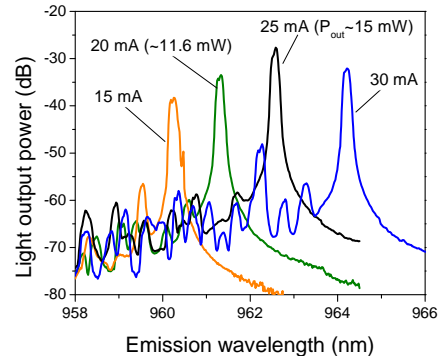

Figure 1. CW 25°C emission spectra for an ~8 μm-oxide aperture diameter VCSEL. The peak single mode optical power is 15 mW with SMSR > 30 dB.
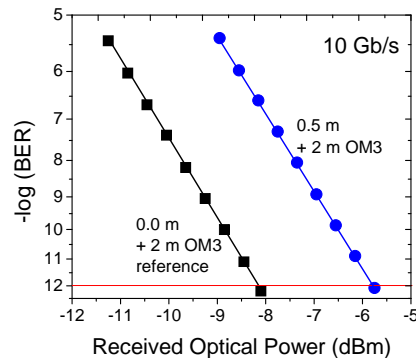

Figure 2. BER at 10 Gb/s at 25°C for a free space optical interconnect (including ~2 m of MMF in the test set up) using an ~960 nm VCSEL.

References
1. M. Gruber, *Applied Optics*, **43**, 463 (2004).
2. M. Grabherr *et al.*, *IEEE PTL*, **10**, 1061 (1998).
3. J.-F. Seurin *et al.*, *Proc. SPIE 6908-7* (2008).
4. R. Safaisini *et al.*, *IEEE JQE,* **46**, 1590 (2010).
5. U. Weichmann *et al.*, *Proc. VCSEL Day* (2013).
6. A. Mutig *et al.*, *Appl. Phys. Lett.*, **97**, 151101 (2010).

Simulations

Session chair : Angélique Rissons

Improved single-mode emission characteristics of long-wavelength wafer-fused vertical-cavity surface-emitting lasers by intra-cavity patterning

N. Volet[1], T. Czyszanowski[2], J. Walczak[2], L. Mutter[1], B. Dwir[1], Z. Micković[1], P. Gallo, V. Iakovlev[1], A. Sirbu[1], A. Caliman[3], A. Mereuta[3], and E. Kapon[1]

[1] *Laboratoire de Physique des Nanostructures, Ecole Polytechnique Fédérale de Lausanne, Switzerland*
[2] *Institute of Physics, Lodz University of Technology, Lodz, Poland*
[3] *BeamExpress S.A., Lausanne, Switzerland*

Keywords: Long-wavelength VCSELs, single-mode emission, wafer fusion, inductively coupled plasma (ICP), three-dimensional numerical model, tomographic image processing.

Current developments in optical fiber communication networks require ever increasing bandwidths and drastic reduction in power consumption of the optical modules involved. Long-wavelength (1.3-1.6 μm) vertical-cavity surface-emitting lasers (VCSELs) offer considerable advantages in these applications over traditional edge-emitting lasers, owing to their easy wavelength setting, low-power consumption, circular beams and low manufacturing costs [1]. The most successful long-wavelength VCSEL technologies employ InP-based structures with strained AlGaInAs quantum wells (QWs) in the active region and a buried tunnel junction (TJ) aperture for current and optical confinement [2, 3]. This has led to room-temperature single-mode (SM) emission powers as high as 6.7 mW, demonstrated with long-wavelength wafer-fused VCSELs [4]. One of the remaining challenges with VCSEL technology is the increase of the SM emission power to the few-milliwatt range for larger temperatures and with acceptable manufacturing yield.

We report on transverse mode discrimination in long-wavelength wafer-fused VCSELs incorporating ring-shaped air gap patterns at the fused interface between the active region and the top distributed Bragg reflector (DBR). These 60-nm deep patterns were implemented with the aim of favoring the fundamental mode while preserving high output power. The VCSELs under consideration emit in the 1310-nm band and incorporate an AlGaInAs-based quantum well active region, a regrown circular tunnel junction and undoped GaAs/AlGaAs DBRs.

A large batch of devices with varying pattern dimensions was investigated by on-wafer mapping, allowing significant statistical analysis leading to conclusions on their typical behavior. We observe experimentally a dependence of the side-mode suppression ratio (SMSR) on the geometrical parameters of the patterns. In particular, we identified

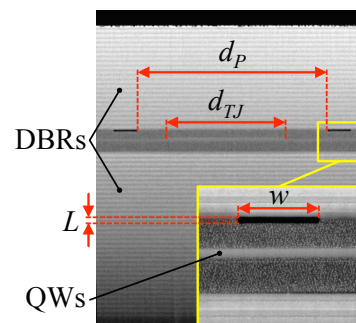a design that statistically increases the maximal single-mode emitted power by more than 20 %.

Figure 1: SEM micrographs showing a vertical cross-section at the center of the device. Inset shows a high-resolution enlargement of the area delimitated by the yellow rectangle.

Numerical simulations of the patterned-cavity VCSELs support these observations. They show that patterns with a large inner diameter actually confine the first-order transverse mode and enhance its modal gain. In smaller devices, this mode is pushed out of the optical aperture and suffers larger losses. Optimized parameters were found numerically for enhancing the single-mode properties of the devices with negligible penalty on emitted power and threshold current.

References

1. A. Larsson and J. S. Gustavsson, VCSELs: Fundamentals, Technology and Applications of Vertical-Cavity Surface-Emitting Lasers (Berlin: Springer, 2013), chap. 4, 119–144.
2. E. Kapon and A. Sirbu, Nat. Photonics **3**, 27–29 (2009).
3. M. Müler, C. Grasse, and M. C. Amann, in 14th ICTON, 1–4 (2012).
5. A. Caliman, *et. al.*, Opt. Express **19**, 16996–17001 (2011).

Scalability challenges of VCSEL-based optical interconnects

W. Hofmann, D. Bimberg.

Institute of Solid State Physics and Center of Nanophotonics, Berlin.

Keywords: Optical interconnects, scalability.

According to IBM, the performance of a single server is going to reach 10 Teraflop by 2020, leading to an aggregated Exa-Byte/s data transport in high-performance computers [1]. These systems can only be realized if the energy consumption of the interconnects is reduced dramatically. "Green IT" has therefore become a crucial subject [2]. We recently evaluated the scalability limits of optical interconnects based on two-dimensional ultra high-speed VCSELs arrays [3]. Future super computers require optical interconnects with accumulated Exa-Byte/s data transport. Arrays of vertical-cavity surface-emitting lasers (VCSELs) might present the only feasible technical solution. Since the whole server will be on a chip, the space is limited by the server die. This translates into optoelectronic devices with a small footprint integrated into a 3D stack on CMOS. One side of the chip will be occupied by the inevitable heat sink; the other side will be needed for the optical IO fan-out. This layout is schematically depicted in Fig. 1. In this configuration, thermal crosstalk becomes dominant with densely packed arrays.
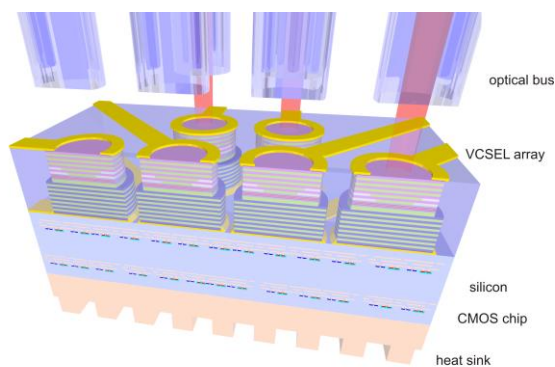

Figure 1. Envisioned schematic layout of a future VCSEL-based optical interconnect based on 3D stacking of optoelectronics on CMOS.

The maximum bandwidth of future VCSEL-based optical interconnects can be derived from the influence of device heating occurring in high-speed VCSEL arrays.

The thermally-limited maximum bandwidth BW_{max} of an optical interconnect based on VCSEL arrays is:

$$BW_{max} = \sqrt{\pi} \cdot \Delta T_{max} \cdot \sqrt{A} \cdot \frac{\lambda}{HBR}$$

With ΔT_{max} as the maximum heating of a device within the array remaining operational, A as the area of the chip, λ as the thermal conductivity of the heat sink and HBR as the heat-to-bitrate ratio:

$$HBR = \frac{P_{diss}}{BR}$$

The dissipated power $P_{diss} = U I - P_{opt}$, with U and I as the VCSELs bias voltage and current, P_{opt} as optical output power and BR as the bit-rate.

We obtain, that VCSEL arrays are highly scalable accommodating the bandwidth density needs of future ultra-dense chip-to-chip optical interconnects. Based on present experimental data, VCSEL-based optical interconnect technology can in principle deliver the highly ambitious 80 Tbps IO bandwidth envisioned for future 10 Teraflop server CPUs. The bandwidth density is scalable from reasonably 100 Gbps/mm² to a physical limit (based on today´s device technology) around 15 Tbps/mm². More energy-efficient devices dissipating less heat are the best solution for scaling the bandwidth up. A high serial bandwidth of the individual channels just helps to keep the number of channels and the complexity of the optical output low, but does not enable higher IO throughput.

References

[1] B. Offrein, "Silicon Photonics Packaging Requirements," IBM Silicon Photonics Workshop, Munich, 23 May 2011 http://www.siliconphotonics.eu/munich_slides/2_IBM.pdf

[2] D. Miller, "Device Requirements for Optical Interconnects to Silicon Chips," Proc. IEEE, vol. 97, pp. 1166-1185, 2009.

[3] W. Hofmann, D. Bimberg, "VCSEL based light sources – Scalability challenges for VCSEL based multi 100 Gb/s systems," IEEE Photonics J., vol. 4, pp. 1831-1843, Oct. 2012.

On-axis pumped VECSEL with double diamond heatspreader

J. Walczak[1], A. K. Sokół[1], M. Gębski[1], V. Iakovlev[2], M. Wasiak[1], M. Dems[1], P. Gallo[2], A. Sirbu[2], E. Kapon[2], T. Czyszanowski[1]

[1] *Institute of Physics, Lodz University of Technology, Wolczanska 219, 90-924 Lodz, Poland*
[2] *Laboratoire de Physique des Nanostructures, Ecole Polytechnique Fédérale de Lausanne, Switzerland*

Keywords: High Contrast Grating, laser, VECSEL.

We present the numerical analysis of optically pumped vertical external cavity surface emitting laser (VECSEL) with improved heat management. In typical VECSELs (Fig.1 – Type1) a single top diamond heat spreader is used in order to redistribute the heat flow to the lateral regions, which allows more efficient transport of the heat to the copper heat sink. We propose further improvement of the heat management by replacing the bottom DBR with a High Contrast Grating (HCG) bounded to the second, bottom diamond heat spreader (Fig.1 – Type2).
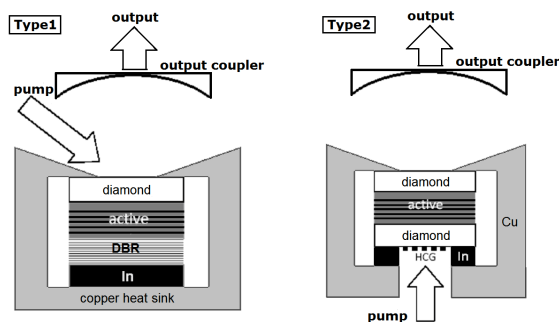

Fig. 1. Two types of VECSEL structures. Type1 is a standard design with the top pumping scheme and single diamond heat spreader and Type2 is the novel design with on-axis bottom pumping scheme and double diamond heat spreader.

Simulations show (Fig.2a) that properly designed silicon HCG deposited on the diamond serves as a high reflecting mirror, assuring reflectivity of 99.999% for the emitted wavelength. On the other hand, HCG reflectivity of the pumping beam (980 nm) is similar to that of diamond and equals ~30%. The proposed new design (Type2), which combines bottom HCG and the on-axis bottom pumping scheme, allows simple and efficient integration with the fiber delivering the pumping beam. We show that the Type2 version allows for the improvement of the thermal impedance by 25% (Fig. 3) and increase of the emitted power by 80% (Fig. 4a) with respect to the Type1 version. As a result of the spectrally narrow peak of the high reflectivity and the polarisation discrimination of the HCG (Fig.2b), Type2 brings also: stable wavelength of the

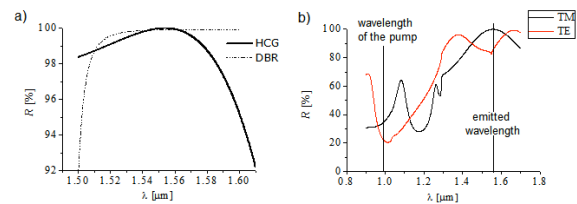emission (Fig.4b) and single polarization of the output beam.

Fig. 2. a) DBR and HCG spectral reflectivity, b) HCG spectral reflectivity for TE and TM polarizations.
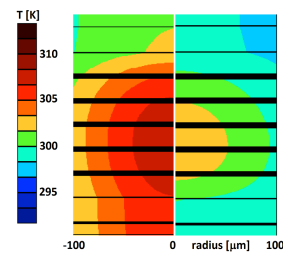

Fig. 3. Temperature distribution in Type1 (left) and Type2 (right) structures. Pumping power is 3W and the ambient temperature is 293.15 K.
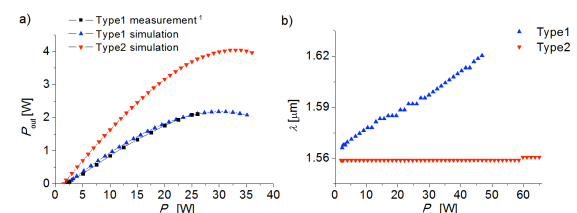

Fig. 4. a) Output power ; and b) emitted wavelength as the functions of the input power for Type1-calculations (blue triangles) and measurements[1] (black squares), Type2-calculations (red triangles).

References

1. A. Sirbu, et. al., *Advances in Optical Technologies*, **2011**, doi:10.1155/2011/209093 (2011).

Acknowledgements

A study of the causes of VCSEL failure under humidity

A.R. Weidberg for the ATLAS Collaboration
Department of Physics, Oxford University, United Kingdom

The ATLAS experiment at CERN has operated a very large number of 12 way oxide aperture VCSEL arrays and experienced very significant failure rates. The optical power for the devices that failed was stable for a timescale of the order of a year and then failed over a period of a few minutes.

This has prompted a major study to identify the main cause of failure and to understand the physics of this failure mode. The first study used accelerated aging tests under conditions of elevated temperature and humidity. This showed that when the VCSELs are powered there was a very large acceleration factor for the aging with relative humidity. Interesting it was found that there was no damage to the VCSELs if they were kept under elevated temperature and humidity for long periods of time when they were not powered. It is well known that oxide aperture VCSELs are sensitive to humidity.

Although we believe we can solve the reliability problems in ATLAS by using VCSEL arrays with dielectric barriers, our experience has led us to try to understand the physics of this failure mode. The results of the accelerated aging tests are combined with those from ATLAS operation to fit the parameters of an acceleration model. In order to try to understand the physics of failure for these devices, we have performed detailed studies on failed and aged but working devices. We have used EBIC and TEM imaging. The EBIC images were used to define the slice to be prepared for a FIB cut and the sample was then imaged with TEM. These images showed the characteristic dense network of dark line defects (DLD) in the MQW active region of the VCSEL. The images also show dislocations that appear to come out of the area near the oxide aperture tip. The plan view also showed a network of DLDs but the damage was too extensive to be able to localise the origin. This analysis is all consistent with the hypothesis that the damage is an electrolytically driven corrosion process that requires the presence of humidity. The damage is believed to start at the oxide aperture and grow towards the MQW layers.

In order to test this corrosion hypothesis, a sample of VCSELs were operated at elevated temperature and high humidity. The optical power was monitored and EL imaging was performed periodically to detect the first signs of damage but before the catastrophic failure occurred. One channel showed a decrease in optical power of 25% and Electroluminescence (EL) imaging showed that 4% of the active areas was dark. Subsequent plan view TEM imaging showed DLDs in this region. Cross sectional TEM images were taken, and then additional thinning was performed, and additional images were taken. These images (see figure 1)
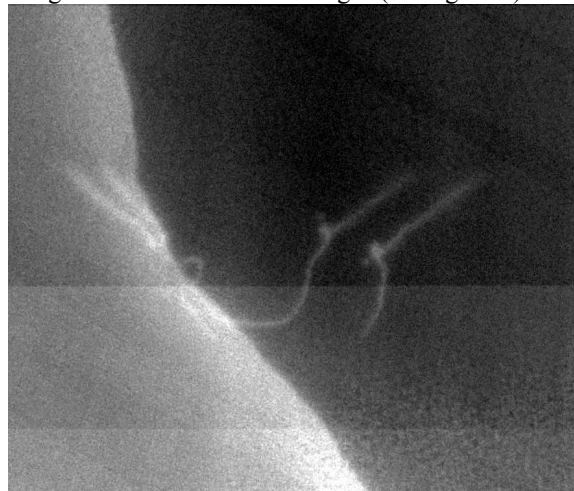

Figure 1 TEM image showing defects originating from the tip of the VCSEL aperture.

showed line dislocations that originated from the oxide tip, near a "loop" feature (that might be a crack). Four line dislocations penetrated into the active region. From these studies we conclude that cracks near the tip of the oxide aperture cause the line dislocations. This is the first published study which shows that the DLDs travel down from the oxide aperture to the active MQW region.

We also found that the spectral width decreased with time for devices operated in normal lab humidity but not for devices operated in dry nitrogen. We have also correlated these studies with microscope near field images. These observations are also consistent with the damage model which will be discussed.

References

1. A. Abdesselam et al., The Optical Links of the ATLAS SemiConductor Tracker, 2007_JINST_2_P09003.
2. VCSEL reliability in ATLAS and development of robust arrays, 2012_JINST_7_C0109.

Spatial mode discrimination in anti-guided arrays of long wavelength VCSELs

Tomasz Czyszanowski[1], Maciej Dems[1], Vladimir Iakovlev[2], Nicolas Volet[2], Eli Kapon[2]

[1] *Institute of Physics, Lodz University of Technology, Wolczanska 219, 90-924 Lodz, Poland*
[2] *Laboratory of Physics of Nanostructures, École Polytechnique Fédérale de Lausanne (EPFL), 1015 Lausanne, Switzerland*

Keywords: Vertical Cavity Surface Emitting Lasers, laser arrays, lateral optical modes

Anti-guided mode schemes are analysed as a confinement mechanism in wafer-fused InAlGaAs/InP 1.3 μm VCSEL arrays (Fig. 1a). The optical apertures are defined by low refractive index ZnSe discs introduced by patterning the interface between the cavity and the top GaAs/AlGaAs DBR. We apply the Plane Wave Admittance Method and perform an exhaustive analysis as a function of the array parameters such as distance between emitters and their aperture size. Fig. 1b presents the modal gains as a function of aperture size for a single emitter. There are two distinct aperture sizes (6 μm and 8 μm), which assure high level of modal gain of the HE_{11} mode.
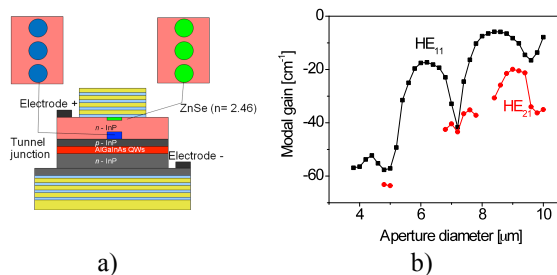

Fig. 1 Modal gains of a single antiguided VCSEL emitter as the function of the optical aperture and schematic view of considered design. 3x1 array is illustrated as an example.

Fig. 2. illustrates the modal gain as the function of the spacing between the emitters for 6 μm apertures for all the modes appearing in 2x1, 3x1 and 4x1 arrays. The 2x1 array reveals the most efficient modal gain discrimination (up to 7 cm^{-1}), however single mode operation occurs for the out-of-phase modes. However, single out-of-phase mode operation is characterised by unwanted multi lobes in far field and large beam divergence angle. Single in-phase mode operation can occur for 3x1 and 4x1 arrays, which produces single lobes in the far field. In those two designs in-phase modes are characterised by larger modal gains with respect to the out-of-phase modes, hence single mode operation occurs only for the in-phase modes. The 4x1 array reveals stronger discrimination with respect to the 3x1 array, which leads to larger

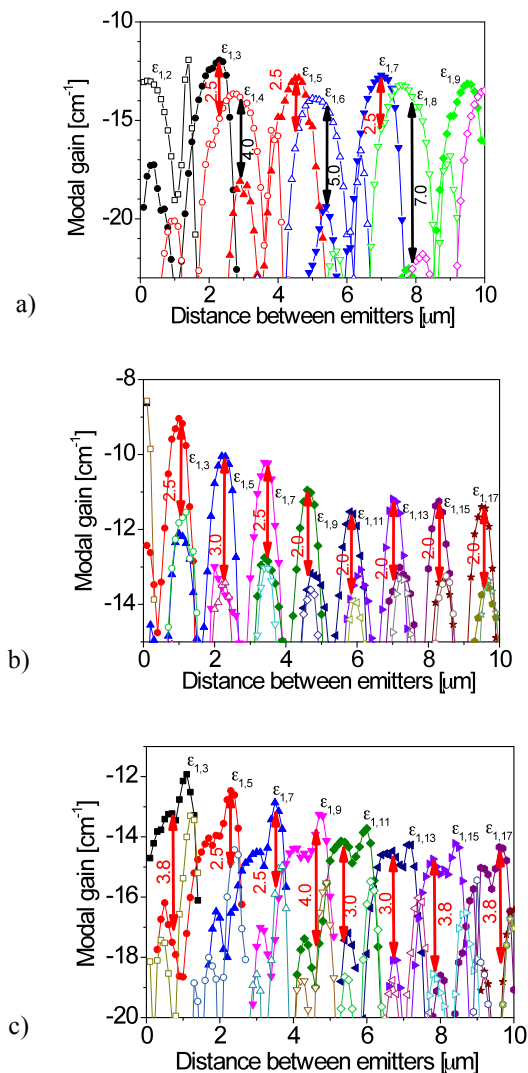emitted power in the single in-phase mode regime of VCSEL array.

Fig. 2 Modal gains vs. distance between emitters for a) 2x1 b) 3x1 and c) 4x1 arrays. Full symbols: in-phase modes, open symbols: out-of-phase modes. Arrows with numbers show the maximal modal discrimination in cm^{-1} for in-phase modes (red) and out-of-phase modes (black).

High contrast gratings

Session chair : Kent Choquette

Hybrid VCSEL using grating mirrors

I.-S. Chung, G. C. Park, Q. Ran, E. Semenova, K. Yvind, and J. Mørk

Department of Photonics Engineering, Technical University of Denmark, DK-2800 Kgs. Lyngby, Denmark

Keywords: High index contrast grating

Increasing power consumption for electrical interconnects between and inside chips is posing a real challenge to continue the performance scaling of processors/computers as predicted by D. Moore. In recent processors, energy consumption for electrical interconnects is half of power supplied and will be 80% in near future. This challenge strongly has motivated replacing electrical interconnects with optical ones even in chip level communications.[1] This chip-level optical interconnects need quite different performance of optoelectronic devices than required for conventional optical communications. For a light source, the energy consumption per sending a bit is required to be <10 fJ/bit for on-chip interconnects and <100 fJ/bit for off-chip interconnects; this is two or three orders of magnitude smaller than the conventional devices. To meet the energy/bit requirement, many innovative laser diode and light-emitting diode (LED) structures have been proposed so far. Our hybrid laser is one of these efforts.[2]

The hybrid laser consists of a dielectric reflector, a III-V semiconductor active material, and a high-index-contrast grating (HCG) reflector formed in the silicon layer of a silicon-on-insulator (SOI) wafer. 'Hybrid' indicates that a III-V active material is wafer-bonded to a silicon SOI wafer. In the hybrid laser, light is vertically amplified between the dielectric and the HCG reflectors, while the light output is laterally emitted to a normal Si ridge waveguide that is connected to the HCG reflector. The HCG works as a vertical mirror as well as a vertical-to-lateral coupler. Very small field penetration into the HCG allows for 3-4 times smaller modal volume than typical vertical-cavity surface-emitting lasers (VCSELs). This leads to high direct modulation speed. Details on device operating mechanism will be explained in the lecture.

References
1. D. Miller, *Proc. IEEE* **97**, 1166 (2009).
2. I.-S. Chung and J. Mørk, *Appl. Phys. Lett*. **97**, 151113 (2010).

GaAs/AlOx and Si/SiO$_2$ high contrast gratings for 980 nm VCSELs

Marcin Gebski[1], Maciej Dems[1], Jian Chen[2], Wang Qijie [2,3], Zhang Dao Hua[2], and Tomasz Czyszanowski[1]

[1]Institute of Physics, Lodz University of Technology 219 Wolczanska str., 90-924 Lodz, Poland

marcin.gebski@p.lodz.pl, maciej.dems@p.lodz.pl, tomasz.czyszanowski@p.lodz.pl

[2]Division of Microelectronics, School of electrical and electronic engineering, Nanyang Technological University,50 Nanyang Ave., 639798, Singapore

[3]Division of Physics and Applied Physics, School of Physical and Mathematical Sciences, Nanyang Technological University, 637371, Singapore, chen0498@e.ntu.edu.sg, edhzhang@ntu.edu.sg, qjwang@ntu.edu.sg

Keywords: Numerical simulations, high contrast gratings, vertical cavity surface emitting lasers.

We present numerical simulations of high contrast grating (HCG) as the potential top mirror of 980 nm VCSEL. We investigate the influence of random nonperiodicity and the absorption of HCG stripes on mirror reflectivity. We determine the maximal fabrication error and the absorption of HCG that still allow to meets the criteria of VCSEL top mirror.
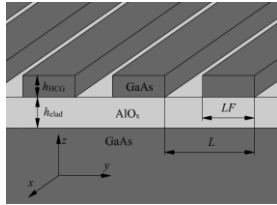

Fig. 1. Simulated HCG structure where L - period, LF - stripe width, h_{clad} - cladding layer thickness, h_{HCG} - grating layer thickness.

The analyzed structure of GaAs/AlO$_x$ HCG is illustrated in Fig. 1. The technological process of HCG etching may introduce the imperfections to the periodic structure of the mirror. We perform the statistical analysis of the standard deviation σ as a measure of manufacturing imperfection of the position of the edges of HCG stripes (Fig. 2).
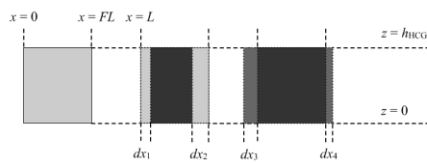

Fig. 2. Randomly disturbed position (dx) of edges of the HCG stripes.

Each point from the maps in Fig. 3 represents the averaged reflectivity over 25 calculations of the same structure, for the same σ with random position of the edges of HCG stripes. σ = 35 nm reduces the reflectivity to the level of 99% which is typical reflectivity of the output mirror of 980 nm VCSELs. Fig. 4 illustrates the influence of the absorption on the HCG reflectivity. We have found that reduction of the reflectivity is linear and very slow varying

with the change of the absorption. The results show that absorption as large as 500 cm^{-1} in HCG stripes allows to reach 99% of reflectivity while typical absorption for GaAs is assumed to be equal to 10 cm^{-1}.
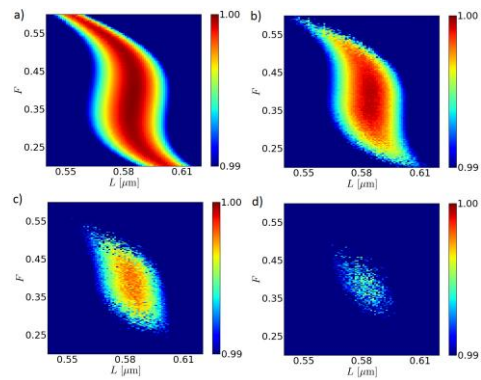

Fig. 3. Maps of HCG reflectivity with respect to period L and fill factor F for standard deviation σ a) 5 nm, b) 15 nm, c) 25 nm, d) 35 nm.
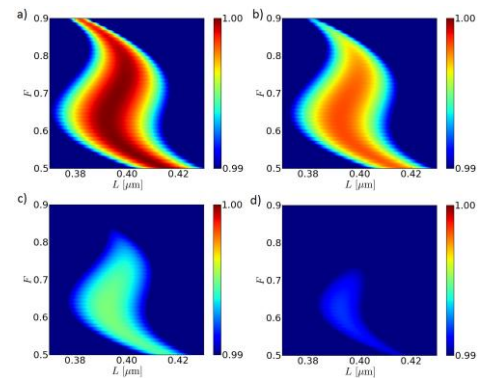

Fig. 4. Maps of HCG reflectivity with respect to period L and fill factor F for absorption in HCG stripes α a) 0 cm^{-1}, b) 100 cm^{-1}, c) 300 cm^{-1}, d) 500 cm^{-1}.

Performance of 980 nm VCSELs with two types of HCGs

P. Debernardi[1], R. Orta[1] and W. Hofmann[2]

[1] *IEIIT-CNR c/o Politecnico di Torino, Corso Duca degli Abruzzi 24, 10129 Torino, Italy*
[2] *Technische Universitaet Berlin, Hardenbergstrasse 36, D-10623 Berlin, Germany*

Keywords: High Contrast Gratings, VCSELs, 3-D vectorial modeling

High Contrast Gratings (HCG) have become a hot research topic, because of their new functionalities at very small volumes [1]. However no efficient 3D VCSEL model capable to account for HCG has been reported to date. HCG design is therefore mainly based on 1D simulations. For more realistic simulations only FDTD has been used so far, which is well known to be computationally very demanding and therefore not usable as a design tool. The VELM code has now been upgraded to rigorously handle HCG layers[2] and improved so as to include also higher order spatial harmonics. In this way one can safely model also structures where those are propagating inside the resonator. The efficiency of the tool is preserved, and an entire set of HCG VCSEL modes can be computed in minutes on an ordinary desktop.
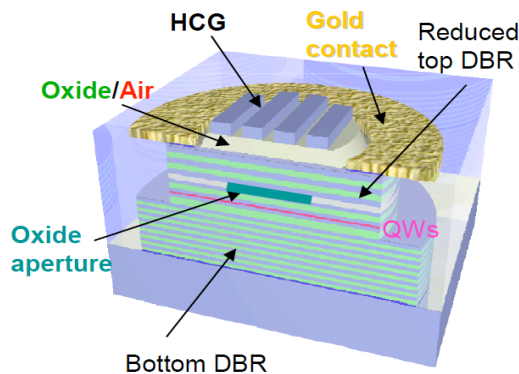

Fig. 1: HCG VCSEL scheme

By exploiting these features, the paper will compare two possible ways of including a HCG in a 980 nm VCSEL. The scheme of the device is shown in Fig.1; it is composed by a GaAs cavity with five 5nm InGaAs quantum wells (QWs) at the center. The back mirror consists of 31 graded $Al_xGa_{1-x}As$ pairs with Al concentration from 0 to 1. The current is injected from the top, through an annular gold ring around the HCG and its oxide-base. To obtain current spreading and confinement, a reduced top DBR is inserted between the cavity and the HCG, which our technology proved to deliver with good quality. Current confinement is achieved by an aperture formed by an in-situ controlled wet oxidation process. These oxide apertures are placed

at a field node, in order to minimize its effect on the field and reduce higher order mode appearance.
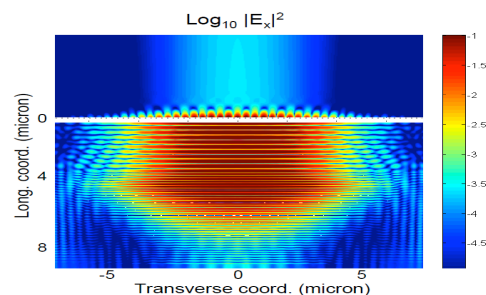

Figure 2: Map of the field profile for 6 μm aperture, HCG on oxide VCSEL.

A full set of design tools, i.e. quasi-1D HCG properties and 3D simulations including the HCG in the VCSEL design, will be presented. In particular two different HCG configurations are considered and compared: a HCG sitting on an AlO_x basement and a free-standing HCG suspended in air, obtained by removing the oxide layer from the optical window. Although the latter technique provides the highest index contrast, the structure with oxide looks more appealing and reliable, because it provides a fully monolithic structure, where the HCG is sitting on an AlO_x layer. For the HCG on oxide, periods as large as 700nm show good performance and easier fabrication. In this case the propagation of first order HCG harmonics in the cavity will be analyzed and discussed. In Fig.1 (at right) the field distribution in the whole device is shown. The propagation of the higher grating order for the oxide VCSEL does not seem to produce too strong effects on the field profile, considering also the use of the logarithmnic scale, and no particular drawbacks appear in the laser operation. The two optimized desing will be compared from the point of view of optical performance: threshold, transverse mode features, near- and far-far field profiles. Technological constraints/feasibility will be addressed and discussed.

References

1. C. J. Chang-Hasnain et al., *Advances in Optics and Photonics* **4** (3), pp. 379-440 (2012).
2. P. Debernardi et al., *IEEE J. Quantum Elect*. **49** (2), pp.137-145, (Feb. 2012)

1.55 μm VCSEL based on InAs quantum-dashes with an emission covering 105 nm wavelength range

F. Taleb[1], **C. Levallois**[1], C. Paranthoen[1], J. P. Gauthier[2], N. Chevalier[1], M. Perrin[1], Y. Leger[1], O. De Sagazan[2], and A. Le Corre[1]

[1]Université Européenne de Bretagne, France, INSA, CNRS-UMR 6082 FOTON, F-35708 Rennes, France
[2]GM-IETR UMR-CNRS 6164, Université de Rennes 1, F-35042 Rennes Cedex, France

Keywords: Quantum-dashes, Wide-gain material, Vertical cavity surface emitting lasers.

We present an InP-VCSEL based on optimized InAs quantum-dashes (QDHs) nanostructures operating at telecommunication wavelength. Contrary to conventional quantum-wells (QWs) based VCSELs, InAs QDHs can be used as gain media in InP-VCSEL to achieve a stable and polarized laser emission[1,2]. Here, we demonstrate an optically-pumped QDH based VCSEL, with a constant and control linear state of polarization, and showing a CW laser emission from 1647 down to 1542 nm, covering thus a spectral window as large as 105 nm. This wide range of lasing wavelength is the result of a wedge microcavity design allowing a spatial dependence of the resonant wavelength along the wafer. This result is an experimental evidence of the large spectral gain of QDH, highly suitable for widely wavelength tunable VCSEL applications. The QDH based active region of our VCSEL is grown by molecular beam epitaxy on a 2 inches diameter InP(001) substrate. This active region consists of three groups of QDHs layers, located at the position of the microcavity antinode fields. Each group corresponds to six InAs QDH layers closely separated with 15 nm $Ga_{0.2}In_{0.8}As_{0.435}P_{0.565}$ barriers. In order to maximize the overall gain, a specific attention has been paid to compensate the natural wavelength shift related to internal strain field, to keep a constant emission wavelength range between each layer and each group of QDH.

The Fig. 1 inset represents the schematic view of the QDH VCSEL including a thick intra-cavity InP phase layer whose thickness decreases from 1500 to 1340 nm from the center up to the edges of the wafer. This thickness variation induces a change in the resonant wavelength as a function of the position on the wafer, as shown in Fig. 1. Laser experiments in CW operation at RT have been performed at different positions on the VCSEL sample. Output spectra have been monitored with an optical spectrum analyzer by moving the pump spot along the radius of the wafer. The different lasing spectra, shown in Fig. 2, have been recorded under 18 mW constant pump power (corresponding to a 10 kW/cm^2 pump power density). Close to the center of the wafer, the lasing wavelength measured is 1647 nm. As the distance from the center increases, lasing wavelength continuously decreases to reach 1542 nm at the edge of the VCSEL sample, demonstrating a CW laser emission at RT in a very large spectral window of 105 nm.

Figure 2. VCSEL output spectra (300K, CW) measured above threshold at a constant pump power, for different position across the wafer (from 5 up to 20 mm, from right to left respectively).
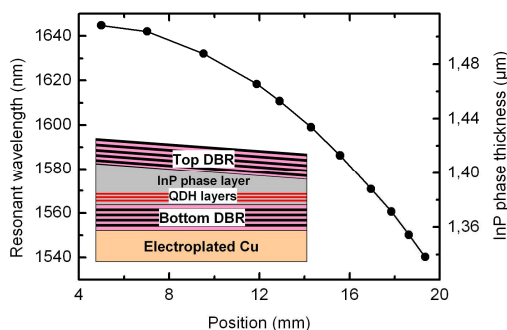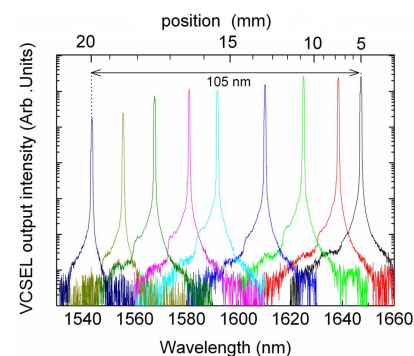

Figure 1. Resonant wavelength of the VCSEL cavity as a function of position on the wafer. Positions indicated in mm correspond to the distance from the wafer center. Inset is a schematic cross-section of the fabricated QDH VCSEL.

References

1. J. M. Lamy *et al*, *Appl. Phys. Lett* **95**, 011117, (2009).
2. J. P. Gauthier *et al*, *Optics Express* **20**, 16832, (2012).

High-Contrast Metastructures for VCSEL Photonics on Silicon

Corrado Sciancalepore[1], Badhise Ben Bakir[2], Sylvie Menezo[2], Xavier Letartre[1], Damien Bordel[2], Pierre Viktorovitch[1]

1- Institut des Nanotechnologies de Lyon, CNRS - Université de Lyon, France
2 - CEA-LETI, Minatec, CEA-Grenoble, Grenoble, France

Keywords: Photonic crystals (PhCs), high-contrast gratings (HCGs), semiconductor lasers, silicon photonics, vertical-cavity-surface-emitting lasers (VCSELs).

High-contrast metastructures can be exploited to perform a controllable spatio-temporal molding of optical features in VCSEL photonics. In detail, the high-index-contrast periodic patterning of the optical medium in photonic crystal membranes (PCMs) can be used for controlling the resonant coupling of radiated light to "heavy photons" states in strongly corrugated waveguides, thus putting photons through a slowed-down transport regime which results in an efficient quasi-3D light harnessing. In the latest years, one-dimensional photonic crystals have been adopted as compact, flexible, and power efficient mirrors in vertical-cavity surface-emitting lasers (VCSELs) emitting in the 850-nm [1] and the C-band [2] wavelength regions, while recently CMOS-compatible VCSEL demonstrators [3], [4] using a double set of Si/SiO_2 PCMs have been realized within a mass-scale fabrication paradigm by employing standard 200-mm microelectronics pilot lines. High fabrication yields obtained via III-V-on-Si molecular wafer bonding [5] of InP-based alloys on silicon conjugate excellent device performances [6] with cost-effective high-throughput production, addressing industrial needs for a fast research-to-market transfer. The extreme flexibility of such innovative photonic architecture enables to perform a fully-controllable transverse mode filtering and polarization control, while the strong near-field mode overlap within mirrors can be exploited to implement unique optical functions such as the optical cavity length trimming for dense wavelength division multiplexing (DWDM) of VCSEL arrays [7, see Fig. 1]. Furthermore, device compactness grants access to a reduced device footprint, power consumption and parasitics, targeting broadband modulation and high-speed data processing. In conclusion, high-contrast gratings are a robust high-performance building block endowing VCSEL optoelectronics with strong perspective potential for several target applications such as high-capacity ultra-wideband optical interconnects, passive optical networks (PONs), high-perfomance computing (HPC), advanced 3-D imaging, free-space data transmission and laser-based sensing.
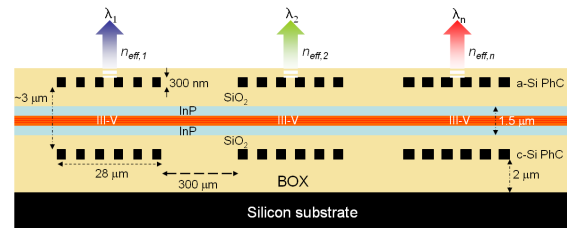

Figure 1 - Schematical view of double PCM-VCSEL arrays enabling on-chip lithographically-addressable wavelength tuning. By trimming the PCM architecture (both fill-factor and period) the modal effective index is modified, inducing a predictable shift in the resonance wavelength.

References

[1] M. C. Y. Huang, Y. Zhou, and C. J. Chang-Hasnain, "A surface-emitting laser incorporating a high-index-contrast subwavelength grating," *Nat. Photonics*, **1**, pp. 119–122, (2007).

[2] S. Boutami, B. Ben Bakir, J.-L. Leclercq, and P. Viktorovitch, "Compact 1.55-μm room-temperature optically pumped VCSEL using photonic crystal mirror," *Electron. Lett*., **43**, pp. 282–283, (2007).

[3] C. Sciancalepore, B. Ben Bakir, X. Letartre, J. Harduin, N. Olivier, C. Seassal, J.-M. Fedeli, and P. Viktorovitch, "CMOS-compatible ultra-compact 1.55-μm emitting VCSEL using double photonic crystal mirrors," *IEEE Photon. Technol. Lett.*, **24**, 6, pp. 455–457, (2012).

[4] C. Sciancalepore, *et al.*, "Quasi-3D light confinement in double photonic crystal reflectors VCSELs for CMOS-compatible integration," *IEEE J. of Lightw. Technol.*, **29**, 13, pp. 2015–2024, (2011).

[5] D. Bordel, *et al.*, "Direct and polymer bonding of III-V to processed silicon-on-insulator for hybrid silicon evanescent lasers fabrication," *ECS Transactions*, **33**, pp. 403-410, (2010).

[6] C. Sciancalepore, B. Ben Bakir, C. Seassal, X. Letartre, J. Harduin, N. Olivier, J.-M. Fedeli, P. Viktorovitch, "Thermal, modal and polarization features of double photonic crystal vertical-cavity surface-emitting lasers," *IEEE Phot. J.*, **04**, 02, pp. 399 - 410, (2012).

[7] C. Sciancalepore, B. Ben Bakir, S. Menezo, X. Letartre, D. Bordel, and P. Viktorovitch, "III-V-on-Si photonic crystal VCSEL arrays for dense wavelength division multiplexing," *IEEE Photon. Technol. Lett*., (*in press*), (2013).

VCSEL with liquid crystal tunable external cavity

Y. Xie,[1] J. Beeckman,[1] K. Panajotov,[2] and K. Neyts[1]

1 Department of Electronics and Information Systems, Ghent University, Ghent 9000, Belgium
2 Department of Applied Physics and Photonics, Vrije Universiteit Brussels, Brussels 1000, Belgium
Keywords: VCSEL, liquid crystal.

We have developed a technology to incorporate thin layers of liquid material on top of VCSELs [1]. The VCSEL is electrically driven and at the same time we are able to apply a voltage over the liquid layer. With this technology we fabricate and characterize an electrically driven VCSEL cell, in which a thin layer of cholesteric liquid crystal (CLC) provides an external optical cavity [2]. We call it CLC-VCSEL. The concentration of the chiral dopant solved in a nematic liquid crystal is chosen such that the material has a reflection band for one circular polarization mode for the emission wavelength of the VCSEL. The properties of the CLC are determined by temperature and can be tuned by changing the temperature. As a result, the emission properties, including threshold current, emission wavelength and polarization states, can be controlled by the temperature.
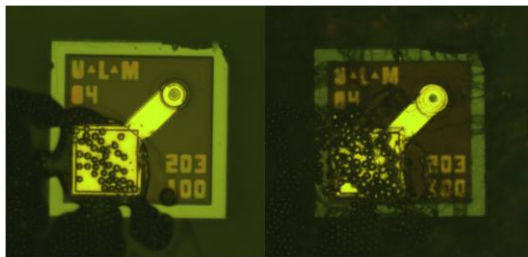

Figure 1. Top view of the reflection microscope pictures of the CLC-VCSEL cell. *Left*: before CLC is filled in; *right*: after CLC is filled in. No polarizer is used for both pictures.

At each temperature point, the optical intensities and emission spectra are investigated at the same time using a beam splitter. The output power is measured as a function of VCSEL current and azimuth angles of a linear polarizer and a quarter wave plate. In this way, the threshold current and the polarization state can be determined. We found that the threshold current of the CLC-VCSEL is smaller than the stand-alone VCSEL at the same temperature. The emission wavelength increases with the temperature. The polarization state of the CLC-VCSEL is a purely circular polarization, rather than linear polarization of a stand-alone VCSEL. By changing the temperature such that the material goes from the nematic liquid crystalline phase to the isotropic phase, the emission can be changes from circularly to linearly polarized.
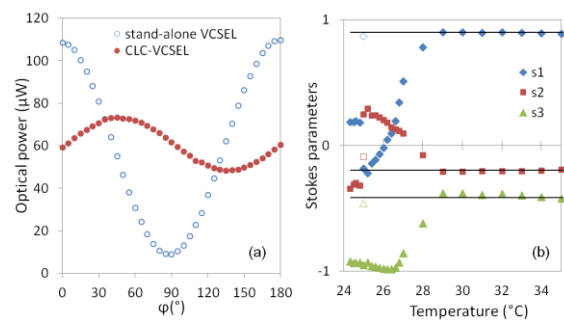

Figure 2. (a) Optical power of stand-alone VCSEL and CLC-VCSEL as a function of azimuth of linear polarizer P at 25°C. (b) The Stokes parameters of the emission at different temperatures (solid dots: CLC-VCSEL, empty dots: stand-alone VCSEL). The Stokes parameters of stand-alone VCSEL at different temperatures are indicated by black lines. VCSEL current is 1.6 mA.

Simulations for the CLC-VCSEL coupled system are studied using a plane wave expansion method [3]. The electric field inside the CLC-VCSEL is calculated along the propagation direction. The simulation result shows that the output light is circularly polarized, which agrees with the measurement. Also simulation indicates the decrease of the threshold due to the increased reflection by the CLC layer.

References

1. Y. Xie, J. Beeckman, W. Woustenborg, K. Panajotov and K. Neyts, *IEEE Photonics Technology Letters* **24**(17), 1509 (2012).
2. K. Panajotov, Y. Xie, M. Dems, C. Belmonte, H. Thienpont, J. Beeckman and K. Neyts, *Laser Physics Letters*, submitted (2013).
3. L. Penninck, J. Beeckman, P. De Visschere, K. Neyts, *Phys. Rev. E* **85**, 041702 (2012).